

Review

The Emergence of the Ubiquity of Cerium in Heterogeneous Oxidation Catalysis Science and Technology

James F. Brazdil

William A. Brookshire Department of Chemical and Biomolecular Engineering, University of Houston, Engineering Building 1, Room S222, 4226 Martin Luther King Boulevard, Houston, TX 77204-4004, USA; james.brazdil@yahoo.com

Abstract: Research into the incorporation of cerium into a diverse range of catalyst systems for a wide spectrum of process chemistries has expanded rapidly. This has been evidenced since about 1980 in the increasing number of both scientific research journals and patent publications that address the application of cerium as a component of a multi-metal oxide system and as a support material for metal catalysts. This review chronicles both the applied and fundamental research into cerium-containing oxide catalysts where cerium's redox activity confers enhanced and new catalytic functionality. Application areas of cerium-containing catalysts include selective oxidation, combustion, NO_x remediation, and the production of sustainable chemicals and materials via bio-based feedstocks, among others. The newfound interest in cerium-containing catalysts stems from the benefits achieved by cerium's inclusion, which include selectivity, activity, and stability. These benefits arise because of cerium's unique combination of chemical and thermal stability, its redox active properties, its ability to stabilize defect structures in multicomponent oxides, and its propensity to stabilize catalytically optimal oxidation states of other multivalent elements. This review surveys the origins and some of the current directions in the research and application of cerium oxide-based catalysts.

Keywords: cerium; cerium oxide; catalyst; oxidation; ammoxidation; combustion; environmental; sustainable



Citation: Brazdil, J.F. The Emergence of the Ubiquity of Cerium in Heterogeneous Oxidation Catalysis Science and Technology. *Catalysts* **2022**, *12*, 959. <https://doi.org/10.3390/catal12090959>

Academic Editors: Yaqiong Su, Jin-Xun Liu and Sen Lin

Received: 4 August 2022

Accepted: 23 August 2022

Published: 29 August 2022

Publisher's Note: MDPI stays neutral with regard to jurisdictional claims in published maps and institutional affiliations.



Copyright: © 2022 by the author. Licensee MDPI, Basel, Switzerland. This article is an open access article distributed under the terms and conditions of the Creative Commons Attribution (CC BY) license (<https://creativecommons.org/licenses/by/4.0/>).

1. Introduction

Virtually every naturally occurring element in the periodic table has found use in heterogeneous catalysis in scientific research and/or commercial applications, even uranium [1–3]. A select subset of elements appear frequently as key catalyst components in one or more catalyzed chemical transformation. Among the members of this subset are platinum and palladium (and recently gold as well has emerged in an increasingly diverse range of catalytic applications) that function as catalysts in their metallic states and are typically supported on a metal oxide—mostly silica and alumina-based, including zeolitic materials. CeO₂ has also become an important support material for metal catalysts because of its ability to impart or promote one or more steps in the catalytic reaction mechanism. For catalysts that effect oxidative chemical transformations, either selective or total, the oxides of molybdenum and vanadium are the most widely cited. In addition, cerium oxide and cerium-containing mixed metal oxides have more recently been found to be potent and useful catalytic materials, especially since about 1980, and have been the subject of extensive literature reviews [4]. Notable among the first applications is the widespread use, and subsequent growth and commercialization, of cerium oxides, specifically cerium–zirconium–oxide solid solutions, in automobile exhaust catalysts as so-called three-way catalysts [5]. Additionally, among the earliest works of this time was that of the author and his co-workers who conducted fundamental and applied research into the incorporation of cerium into solid solutions of molybdate-based catalysts for the ammoxidation of propene to acrylonitrile [6]. This work will be described more in this

review. The common link between many of these initial studies was the aspiration to exploit the redox capability, oxygen content variability, and surface oxygen activation of cerium oxides and cerium-containing oxide solid solutions.

By the 1990s and beyond, an exponential growth occurred in research (as evidenced by the number of scientific publications) and application (as evidenced by the number of patent publications) of cerium in oxide-based catalysts. This trend is documented in Figure 1, which shows the number of cerium oxide catalyst publications compared to the number of publications for the quintessential oxidation catalyst components of molybdenum and vanadium. The oxides of molybdenum and vanadium had been in wide use before 1980 as effective catalysts for a range of oxidation processes with various feedstocks that included low molecular weight alkenes and alkanes as well as several methyl-substituted aromatic feedstocks [7].

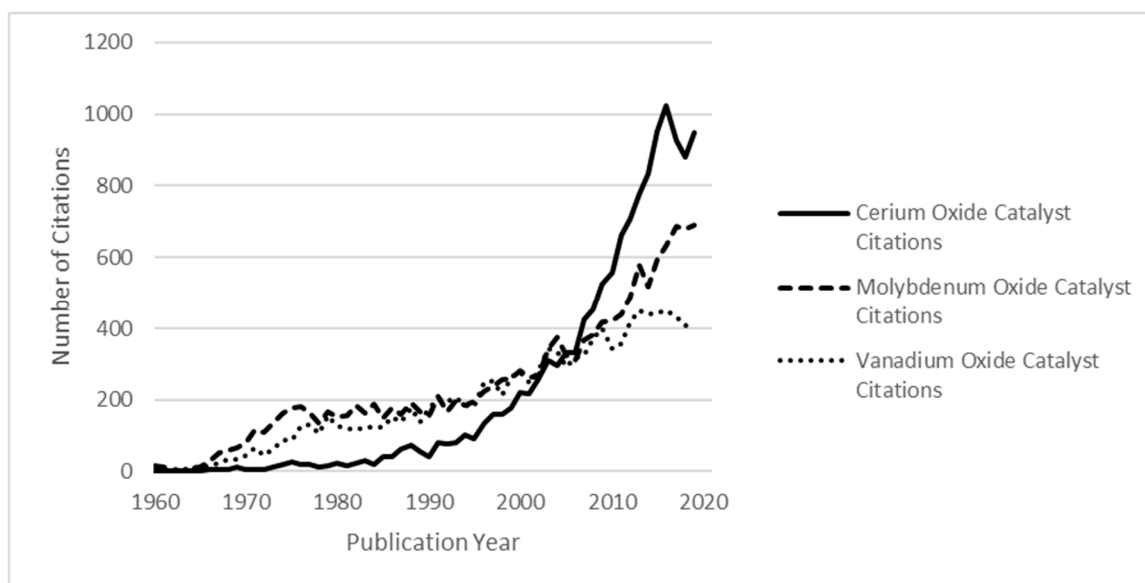


Figure 1. Publications per year on cerium, molybdenum, and vanadium-containing catalysts. Source: SciFinder.

This review examines the expanding application of cerium oxide-containing catalysts with a focus on chemical transformation that exploit the specific redox chemistry of cerium—most notably in catalyzing oxidation reactions. This can entail cerium oxide as a specific catalytically active component or as a nominal support material. More frequently, it is the ability of cerium to form solid solutions with various metal oxide structures that permits the incorporation of its redox activity in close proximity to other elements that are key to catalyzing critical steps in the overall reaction mechanism. This review also examines other physical and chemical properties of cerium that have proven catalytically beneficial and have placed cerium as a key element in the pantheon of catalysis science and technology.

2. Application of Cerium in Oxidation Catalysts

2.1. General

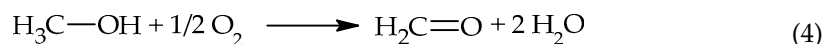
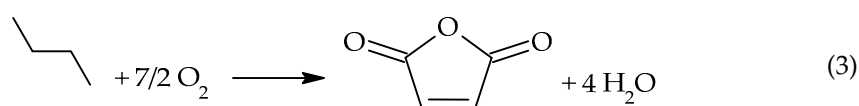
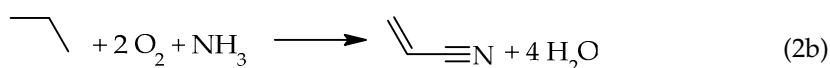
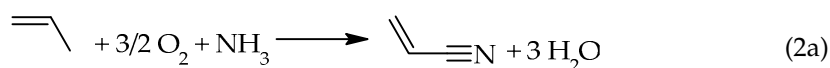
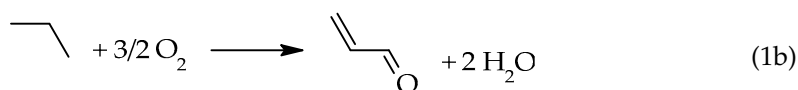
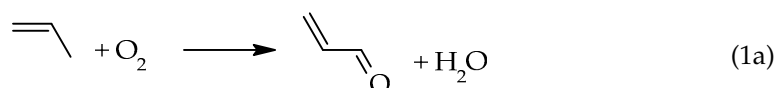
Catalytic oxidation can be categorized either as partial oxidation (i.e., selective) or total oxidation (i.e., combustion) to CO_2 . The oxidation reaction can be effected by catalysts that function through several established reaction mechanisms. Total oxidation typically is initiated by the reaction with active surface adsorbed oxygen species, such as O^- or O_2^- . This typically proceeds by the Eley–Rideal mechanism in which the adsorbed active oxygen species reacts with a reactant that is not chemisorbed on the catalyst surface but is present in the gas phase [8]. Selective oxidation typically proceeds by the Mars–van Krevelen mechanism [9], wherein lattice oxygen, O^{2-} , is the catalytically active moiety

responsible for activation of an adsorbed reactant and/or is the species inserted into the reactant and incorporated into the final product(s). This lattice oxygen is removed in the course of the reaction and the resulting oxygen vacancy is replenished by the diffusion of lattice oxygen from the bulk and then ultimately replaced at a separate, reoxidation site, where O_2 is reduced to O^{2-} . Cerium-containing oxides have been shown to be effective catalysts across both classes of oxidation mechanisms because of the combination of their unique capability to form surface oxygen vacancies and their proficient redox chemistry of shuttling between the two stable oxidation states of Ce^{3+} and Ce^{4+} .

2.2. Selective Oxidation Applications

Although arguably the Haber–Bosch process for the industrial manufacture of ammonia is the most significant invention to benefit humankind and is a catalytic process at heart, selective oxidation and ammoxidation of propene to produce acrolein, acrylic acid, and acrylonitrile is no less a technological marvel of catalysis science. The follow-on science has produced some of the greatest advances in the understanding of catalytic phenomena.

Selective oxidation catalysis encompasses several commercially important chemical transformations. Based on commercial application and research interest, the most important reactions, shown below, are the oxidation of propene and propane (not commercial) to acrolein (1a, 1b), ammoxidation of propene and propane to acrylonitrile (2a, 2b), butane oxidation to malic anhydride (3), and methanol oxidation to formaldehyde (4).



The catalysts for these chemical processes were initially developed based on mixed metal oxides that contained molybdenum and/or vanadium. Thus, these basic catalytic processes were developed largely before the rapid growth of research into improving these oxide catalyst systems with the incorporation of cerium. Subsequently, significant benefits were realized in activity, yield, and selectivity. This review includes a discussion of these processes, and other oxidations, with respect to the improvements obtained via cerium incorporation into catalyst formulations.

2.2.1. Propene and Propane Selective Oxidation to Acrolein

Bismuth–molybdenum–oxide is the ubiquitous active component of catalysts for the selective oxidation of propene and isobutene to acrolein and methacrolein, respectively. It is the essential active phase for virtually all commercial catalysts for production of acrolein, which is then converted to acrylic acid in a second step using a compositionally different catalyst based on molybdenum–vanadium oxide. The addition of rare earth elements,

especially cerium, as catalyst components has become increasingly prevalent in these formulations because it provides improved product yields and catalyst stability [10–12].

Bismuth molybdate exists in three crystallographic structures commonly denoted as α - $\text{Bi}_2\text{Mo}_3\text{O}_{12}$, β - $\text{Bi}_2\text{Mo}_2\text{O}_9$, and γ - Bi_2MoO_6 . Their structures have been well characterized as well as their catalytic behavior for selective alkene oxidation [13–15]. The development of improved catalysts with higher activity and selectivity to partial oxidation products focused on promotion by transition metals, most notably iron, cobalt, and nickel [16–18]. Further improvements were achieved with the doping of the alkali metals potassium, cesium, and rubidium [19]. These promoter elements are present in the multicomponent catalyst in the following crystallographic phases:

- Divalent $\text{M}^{2+}\text{MoO}_4$ molybdates of the α and/or β structure type in which M^{2+} is one or more of Ni^{2+} , Co^{2+} , Mg^{2+} , Fe^{2+} typically as a single solid solution.
- Trivalent $\text{Fe}_2\text{Mo}_3\text{O}_{12}$.

Bismuth molybdate is invariably present as the α - $\text{Bi}_2\text{Mo}_3\text{O}_{12}$ structure type.

Cerium was a relative newcomer to this development work. The primary role of cerium has been identified as augmenting the function of the redox active phases, which comprise iron in the Fe^{2+} and Fe^{3+} oxidation states [20]. The role of these phases is to maintain the active site components, bismuth and molybdenum, in their highest oxidation states that are most conducive to optimal acrolein yield. The redox elements are thought also to serve as the sites for gas phase oxygen reduction and the incorporation of lattice oxygen (reoxidation). These functionalities ensure the long-term operability and stability of the catalyst during the course of the surface reaction mechanism. The promoting effect of cerium in a bismuth molybdate catalyst for selective propene oxidation to acrolein is exemplified in Table 1.

Table 1. Promoting the effect of cerium addition to a bismuth molybdate catalyst for selective oxidation of propene to acrolein [20].

Wt.% Ce in BiMoOxide	% Propene Conversion	% Acrolein Selectivity	% Acrolein Yield
0	81.6	70.7	57.7
1	78.2	72.1	56.4
3	78.6	73.8	58.0
5	82.7	73.5	60.8
10	86.0	75.7	65.1

The innate price advantage of propane compared to propene prompted extensive industrial research into a catalytic process to replace propene with propane for producing acrolein as the intermediate for acrylic acid manufacture. The earliest catalyst design strategy was to look at modifying the known bismuth molybdate catalyst by including elemental components, such as vanadium, that are known to be effective in activating an alkane. This creates a dual function catalyst that first converts propane to propene as a reaction intermediate and then relies on the bismuth molybdate component as a co-catalyst to convert the propene to acrolein. In such a catalyst system, the redox activity of cerium was also found to be of benefit [21]. The cerium addition translated into the higher overall activity of the catalyst, and it was interpreted that the presence of cerium provides more active lattice oxygens for oxidation as cerium replaces bismuth in the active phase of the catalyst.

Other multicomponent oxides have also been identified for selective propane oxidation. One such catalyst comprises Ag-Mo-P-O wherein cerium was found to be effective as a redox promoter [22,23]. In this case, the promotion of cerium was seen to manifest in the creation of reduced molybdenum sites that were viewed to be critical for the activation of propane via the following redox reaction.



The same cost incentive mentioned above exists for developing a propane-based process for producing acrylonitrile. The catalyst research on a propane-based acrylonitrile process took a parallel path to the work on propane oxidation to acrolein with essentially identical oxide catalyst systems investigated for both processes. It was, however, only in the case of producing acrylonitrile that a successful and commercially viable process was eventually developed. The reason for this is severalfold. From a strictly technical and scientific perspective, the activation of an alkane versus an alkene by hydrogen abstraction on a catalyst surface is more energy intensive with respect to the strength of the C-H bond to be broken. Therefore, an alkane conversion process is typically expected to require either/or both harsher (higher temperature) conditions and catalysts that contain active elements with higher intrinsic oxidation activity than required for selective alkene oxidation. Because of the latter and because acrolein is more reactive (less stable to oxidative degradation) than acrylonitrile, such conditions and catalysts will typically result in consecutive oxidation of acrolein to CO and CO₂ thus greatly limiting the potential for achieving the high yields and efficiency necessary for a commercial operation. A further impediment to a commercial propane-to-acrolein process is the fact that current industrial propene-to-acrolein process technology approaches 90% acrolein yields with the acrolein plus acrylic acid at more than 90% [24] effectively presenting an insurmountable hurdle to achieve the necessary acrolein yields for commercial competitiveness with propene-to-acrolein technology. So, most of the research and development effort has been focused on propane ammoxidation to acrylonitrile and it is in this context that cerium was identified as a beneficial component in the most successful oxide catalyst system as discussed below.

2.2.2. Selective Ammoxidation of Propene and Propane to Acrylonitrile

Catalytic selective ammoxidation entails a wide spectrum of commercially important chemical transformations that encompass the conversion of C₃ and C₄ alkenes and alkanes to corresponding unsaturated nitriles and the conversion of methyl substituted aromatics to the corresponding aromatic nitriles. The most important industrially, based on worldwide production of around seven million metric tons per year (7000 kt/a), is the production of acrylonitrile by the ammoxidation of propene via the SOHIO process [25].

The first scientifically and technically significant investigation of cerium in a selective oxidation catalyst was for propene ammoxidation to produce acrylonitrile. Although bismuth-phospho-molybdate was the first catalyst discovered, developed, and commercialized for the propene ammoxidation SOHIO Process [26,27], this revolutionary catalytic technology immediately sparked a global research effort to develop alternative catalysts for industrial application. Among the earliest of these alternative catalyst formulations was a cerium-containing mixed oxide catalyst with tellurium and molybdenum [28–32]. The characterization of this catalyst system revealed a complex mixture of known metal oxide phases but also several distinct cerium-containing phases. It was the presence of a unique ternary Te-Ce-Mo oxide (Ce₄Mo₁₀Te₁₁O₅₉), coexisting with separate cerium molybdate phases seen for the first time, that was responsible for its effectiveness in the selective ammoxidation of propene. The role of cerium in promoting the selective ammoxidation reaction was attributed to the co-existence of cerium with other catalytically active metals. Critical to the performance enhancements obtained with these catalysts is the ability of cerium to facilitate reoxidation of molybdenum.



Maintaining molybdenum in its highest oxidation state under catalytic conditions is also necessary for catalyst stability. This provides structural integrity of the catalyst during the redox operation of the catalyst by preventing reductive phase formation and the resulting phase segregation that typically results in the degradation of catalytic activity and selectivity.

The incorporation of the redox properties of cerium into bismuth molybdate-based acrylonitrile catalysts proved to be highly successful from a commercial standpoint but

also scientifically as much has been learned about the solid-state mechanism of selective (amm)oxidation catalysis from the work. Specifically, this work provided validation and new insights into two of the most successful catalyst design strategies used by researchers in the development of new and improved catalyst systems:

1. Solid solution/single phase formation within the catalytically active phase.
2. Synergistic phase interaction (most effectively via structural epitaxy).

The cerium doping of a bismuth molybdate oxidation catalyst was first reported in the 1980s with the disclosure of the “Bi₉CeMo₁₂O₅₂” composition as an effective catalyst for propene ammoxidation [33]. Additional investigations into cerium addition to bismuth molybdate catalysts followed [34–37]. This culminated in the incorporation of cerium in numerous patents as a constituent of complex multicomponent catalysts designed for commercial application [38–43]. It was discovered that the bismuth molybdate scheelite structure is able to accommodate the redox-active element cerium. Enhanced catalytic activity and selectivity is enabled by the Ce³⁺/Ce⁴⁺ redox couple at the atomic level in the direct vicinity of catalytically essential components bismuth and molybdenum necessary for the activation of propene via α -H abstraction and subsequent oxygen/nitrogen insertion. Thus, the redox-active cerium promoter functions within the same structural phase as catalytically active components bismuth and molybdenum. The redox activity of cerium has also been invoked for preventing the sublimation of molybdenum from multiphasic molybdate catalysts during operation [44].

The bismuth–cerium molybdate solid solution active phase has been shown to be directly amenable to a range of promoter elements that, in the case of propene ammoxidation to acrylonitrile, increase product yield from around 65% to over 80%. The most effective promoters are tungsten, antimony, potassium, and cesium, as shown in Table 2.

Table 2. Promoting effect of bismuth–cerium molybdate propene ammoxidation catalyst system (See reference for specific reaction conditions) [45].

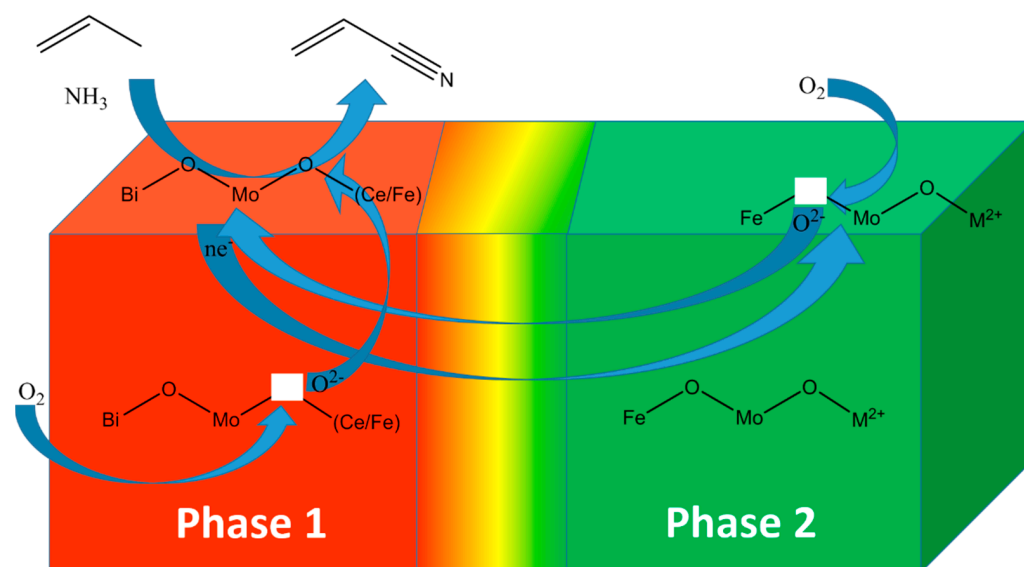
Catalyst Composition	Reaction Temperature (°C)	% Propene Conversion	% Acrylonitrile Yield
Bi ₄ Ce ₄ Mo ₁₂ O _x	430	100	65.8
	460	100	71.5
Bi ₄ Ce ₄ Mo ₁₀ W ₂ O _x	430	98.6	69.5
K _{0.1} Bi ₄ Ce ₄ Mo ₁₂ O _x	460	99.3	79.8
Cs _{0.02} Bi ₄ Ce ₄ Mo ₁₂ O _x	445	98.4	74.4
Cs _{0.04} Bi ₄ Ce ₄ Mo ₈ W ₄ O _x	460	99.5	81.8
Cs _{0.04} Bi ₄ Ce ₄ SbMo ₁₀ W ₂ O _x	460	97.9	80.0

The bismuth–cerium molybdate active phase has also been shown to be effective when in combination with the typical components of commercial acrylonitrile catalysts, including iron, cobalt, nickel, magnesium, and alkali metals. These are multiphasic oxides of the type described above for propene oxidation to acrolein and related compositions have been disclosed for the manufacture of acrylonitrile. The bismuth–cerium molybdate active phase can also be promoted by other multivalent rare earth cations, such as samarium, praseodymium, and neodymium, which have a similar cation size to cerium, via solid solution formation. The catalysts of this type have achieved acrylonitrile yields from propene of as high as 86% [46], as shown in Table 3.

Table 3. Examples of cerium in high-performing silica-supported industrial acrylonitrile oxide catalyst formulations.

Elements						% Acrylonitrile Yield
Cs	Co	Fe	Bi		Mo	76.3 [47]
Cs	Co	Fe	Bi	Ce	Mo	86.4 [47]
Rb	Co Ni Mg	Fe	Bi	Ce	Mo	86.0 [47]
Cs	Co	Fe	Bi	Pr	Mo	85.7 [47]
Rb	Ni Mg	Fe Cr	Bi	Ce Sm	Mo	85.8 [46]

As shown in Figure 2, the understanding of the solid-state mechanism of the single-phase model catalysts has augmented the understanding of the industrially important multiphase cerium-containing oxide selective ammoxidation catalyst systems as well [48].

**Figure 2.** Schematic representation of multifunctionality in single and multiphase in an ammoxidation catalyst system [48].

Using this conceptual phase composition model as a catalyst design strategy, major commercial acrylonitrile producers have identified compositional spaces for catalysts to provide optimal yields of acrylonitrile from propene [49–52]. In most cases, these catalyst development efforts entailed the rigorous solid-state structural characterization of complex multicomponent oxides. Critical information regarding the quantification of phase compositions via Rietveld X-ray diffraction methods was obtained and related to the performance of the catalyst with respect to acrylonitrile yield from propene, as shown in Figure 3, for several cerium-containing multicomponent metal oxide catalysts.

The success in providing the best-performing, state-of-the-art cerium-containing commercial acrylonitrile catalysts is the validation of the practicality of this conceptual redox model.

For the development of catalysts and processes to replace propene with propane as a lower cost feedstock for commercial acrylonitrile manufacture, numerous mixed metal oxides have been explored in both industrial and academic laboratories. The catalyst system that was found to be the most conducive to retrofitting existing propene ammoxidation process technology appeared in a series of patent disclosures by Mitsubishi Chemical Company in the 1990s. These patent disclosures reported that a new type of catalyst formulation combined with a distinct preparation method produced a catalyst providing both high propane conversions (i.e., 80% to 90%) along with relatively high yields of acrylonitrile (i.e., up to 59%) [53]. The publication of these patent disclosures inspired numerous worldwide research programs that have produced a large number of published

academic research articles describing fundamental studies of the catalyst formulations. Among the many findings of these research efforts was that cerium effectively promotes the increase in the yield of acrylonitrile from propane for a Mo-V-Te-Nb mixed oxide catalyst [54]. The conclusion from the work was that the promotion effect of cerium is in fact multidimensional. Cerium was shown to be a solid-state structural promoter by increasing the amount of the catalytically critical M1 phase [55–57] in the catalyst. The overall result is a relatively higher concentration of Te^{4+} on the catalyst surface. Tellurium has been found to be a critical component of the catalyst as it is likely responsible for the selective conversion of the intermediate propene produced from propane to acrylonitrile [58]. The Te^{4+} moiety in this oxide matrix has also been proposed from modeling studies as being responsible for the rate determining step of propane activation via hydrogen abstraction [59].

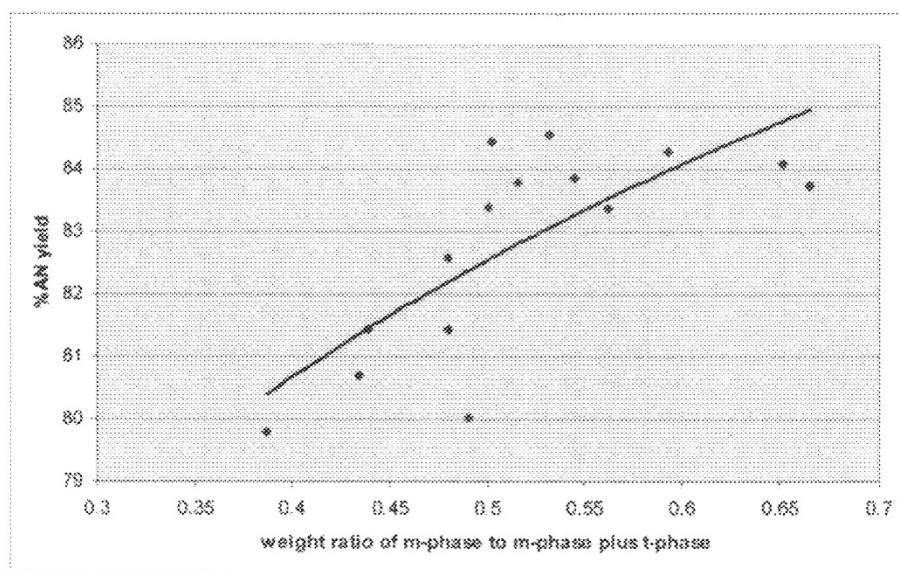


Figure 3. Rietveld X-ray diffraction analysis of cerium-containing mixed metal oxide acrylonitrile catalyst where m-phase ($\text{Ce}_2(\text{MoO}_4)_3$) and t-phase refer to the monoclinic and tetragonal forms of the scheelite structure, respectively [49].

The Japanese chemical manufacturer Asahi exploited the breakthrough in the propane ammoxidation catalyst formulation by commercializing a cerium promoted variant for acrylonitrile manufacture. The successful scale up is evidenced from a patent publication with a catalyst formulation consisting of $\text{Mo}_1\text{V}_{0.21}\text{Nb}_{0.09}\text{Sb}_{0.25}\text{Ce}_{0.005}\text{O}_x/45 \text{ wt\%}-\text{SiO}_2$ and operation in a commercial scale 8 m diameter fluid-bed reactor with acrylonitrile yield from propane of 52% [60]. Asahi successfully constructed a new-build propane-to-acrylonitrile plant based on this catalyst type [61]. The highest acrylonitrile yield reported with the cerium-containing catalyst formulation apparently used in the Asahi plant is around 56% [62].

The 56% to 58% acrylonitrile yield from propane may indicate an economic advantage over an 85% acrylonitrile yield from propene depending on propane/propene pricing. However, based on an analysis of economic cases for propane versus propene as a commercial feedstock for acrylonitrile, a propane-to-acrylonitrile yield closer to 70% is more likely required for a complete retrofitting of existing propene-based commercial plants [63].

2.2.3. Butane Oxidation to Maleic Anhydride

One of the earliest studies to examine the possible benefit of cerium promotion in a VPO catalyst for butane oxidation to maleic anhydride concluded that the increased yield of maleic anhydride observed with the promoted catalyst (co-promoted with molybdenum) was due to added redox stability that prevented reduction in the catalytically active V^{4+} [64,65]. The VPO_x active phase for the catalytic conversion of butane to maleic

anhydride is unique in the selective oxidation field. It requires a precise method of catalyst preparation and activation to generate the correct catalytically active phase to produce maleic anhydride. It is not generally amenable to the addition of promoter elements as it does not form continuous solid solutions with other cation species. The scientific and technical literature has, thus, focused mostly on the preparative chemistry of the VPO_x as it has been observed to have a significant impact on the catalytic properties of the operating catalyst. Nevertheless, the paucity of reported results with additives may provide an opportunity to explore the logical inference of redox promotion of the catalyst by the proper synthetic incorporation of multivalent elements, including cerium.

2.2.4. Oxidative Dehydrogenation

The production of alkenes from alkane feedstocks by oxidative dehydrogenation (ODH) in a continuous single-pass process that co-feeds oxygen (air) with the alkane offers the potential commercial advantage of both high conversion and high yield without the thermodynamic yield limitation for the alkene product of a non-oxidative process that produces H_2 as a coproduct. A single-pass process would also simplify current commercial cyclic processes that entail two process steps of catalytic reaction followed by catalyst regeneration with an O_2 containing gas. The single-pass, high-conversion process for alkane ODH has not reached commercial viability because of a fundamental limitation on alkene yield observed with catalysts studied to date. This is due to the consecutive oxidation of the alkene product to CO and CO_2 in the surface reaction mechanism. As can be seen in the following reaction network, if k_3 is a significant value compared to k_1 and k_2 , there is a kinetic limitation to the amount of alkene that is possible at high alkane conversion levels.



Although many transition metal oxides have been studied as catalysts for ODH, the primary focus has been on oxides containing vanadium and/or chromium because their oxides are known to be effective agents for the catalytic activation of alkanes via hydrogen abstraction in the initial rate determining step [66,67]. Building on this base of understanding, oxide-based catalysts promoted with cerium have been extensively evaluated for the oxidative dehydrogenation of C_2 - C_4 alkanes [68].

The Mo-V-Te-Nb mixed oxide catalyst described above for the ammoxidation of propane to acrylonitrile is also extremely effective as a catalyst for the ODH of ethane to ethene. An extensive reaction and characterization study was reported on the effect of cerium addition to this catalyst system [69]. Cerium proved to be a powerful promoter element by increasing the activity of the catalyst and enhancing the yield of ethene from ethane, as shown in Figure 4. Not surprising for the incorporation of a promoter element to a catalyst is that there is an optimum in the level of the promoter that achieves the best overall performance in terms of activity and product yield.

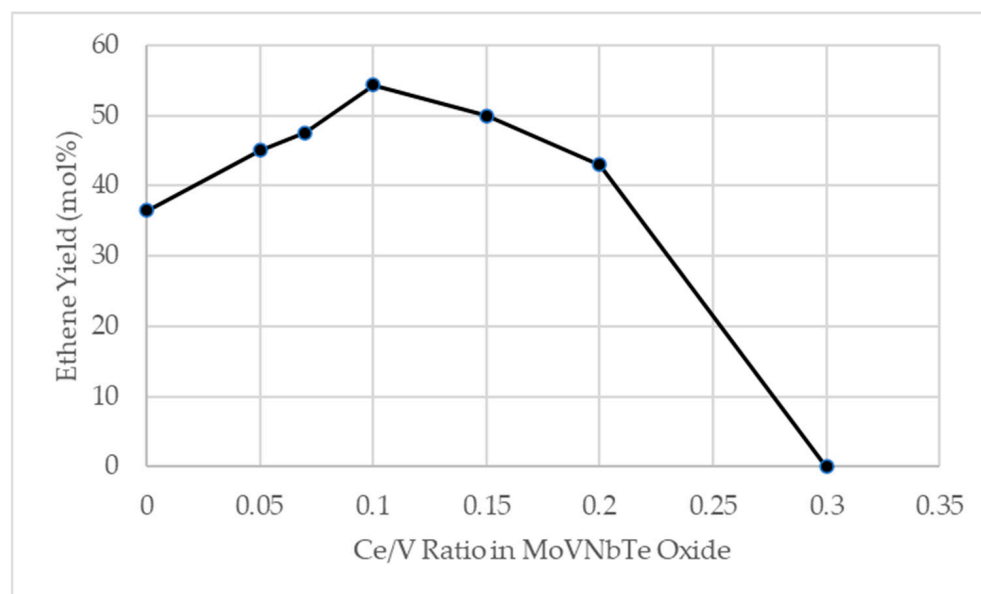


Figure 4. Ethane ODH with MoVTeNb Oxide catalyst with varying levels of cerium content. Source [69].

The characterization study concluded that the performance improvement achieved by the addition of cerium was due to multiple effects by the additive:

1. Cerium is directly incorporated into the active phase as evidenced by the X-ray diffraction analysis showing a monotonic increase in unit cell volume of the active M1 crystal phase of MoVNbTeO_x (PDF 00-058-0789) with increasing cerium content.
2. The redox activity of cerium promotes the stabilization of the high oxidation state of the active catalyst moiety—in this case, the V^{5+} —by promoting the replacement of lattice oxygen in accordance with the operative Mars–van Krevelen mechanism for the reaction.
3. Cerium increases the amount of lattice oxygen available, and thus the reducibility of the catalyst, for the reaction, which is manifested in the enhanced activity of the catalyst.

The selective oxidative dehydrogenation of 1-butene to 1,3-butadiene has been shown to benefit from the addition of cerium to bismuth molybdate [70]. The characterization of the cerium-containing bismuth molybdate found that cerium enhances the catalytic performance by increasing oxygen mobility and adsorption of 1-butene. The observed ceric molybdate phase was seen as the oxygen donor phase with the bismuth molybdate phase the oxygen acceptor in the ODH reaction. The ODH of ethane to ethene has been shown to be similarly benefited by the presence of the $\text{C}^{3+}/\text{Ce}^{4+}$ redox couple in VO_x/CeO_2 catalysts in the context of the VCeO_4 active phase to stabilize and re-oxidize the $\text{V}^{5+}\text{-O-Ce}^{3+}$ active site [71].

2.2.5. Other Selective Oxidation Reactions

The selective catalytic oxidation of methanol is a commercially important technology for the manufacture of formaldehyde. The most widely used process technology incorporates iron molybdate and vanadium oxide-based catalysts to effect the chemical transformation. Similar to other selective oxidation processes discussed herein, the catalytic mechanism involves a redox process within the oxide catalyst with the direct involvement of surface and lattice oxygens of the solid oxide catalyst. Thus, the facile charge transfer among the multivalent constituents of the catalyst, namely vanadium, iron and/or molybdenum, must occur. For this reason, cerium has been identified as a beneficial promoter by enhancing this requisite redox function in the catalyst.

In the case of ceria-supported vanadium oxide catalysts, ref. [72] characterization and computational studies show the promoting effect of cerium is as other oxidation catalysts, with the source of the promotion both structural and redox related. Specifically, electron transfer to the f electronic states of cerium to produce Ce^{3+} in the CeO_2 support keeps the catalytically active vanadium surface site in the fully oxidized 5+ state [73,74]. In addition to the redox promotion, the increased activity of the ceria-supported catalyst was due to the resulting oxygen vacancies serving as sites for methanol adsorption and hydrogen transfer [75]. A structural-based promotion by ceria is evident from high-resolution photoelectron spectroscopy and infrared spectroscopic characterization, which show the reducible ceria support isolates and stabilizes the V=O species responsible for high activity and selectivity for hydrogen abstraction and oxidation of methanol to formaldehyde [76].

Increasingly, evidence is being produced that cerium oxide can also have a direct role in the surface mechanism of chemical transformations, such as direct hydrogen abstraction [77], structure sensitivity (with the CeO_2 (111) crystal face providing highest selectivity [78]), and the stabilization of formate intermediate species during catalytic decomposition of methanol [79,80] (the CeO_2 (100) crystal face being preferred [81]).

Another application of a cerium-containing oxide catalyst is for the selective ammoxidation of methanol to HCN [82]. Although most of the commercial HCN produced is a co-product of the propene ammoxidation process, on-purpose HCN production is an important commercial technology to augment the supply of this important chemical intermediate. This application further highlights the redox role of cerium to affect the efficiency of a bismuth molybdate active phase. As described above, other rare earth elements can isomorphously occupy the same crystalline site that bismuth occupies in the scheelite structure. As shown in Table 4, when lanthanum, which only exists as a 3+ cation, is incorporated into the structure, the overall yield of HCN is significantly less than when the redox active cerium cation (which can exist in the 3+ or 4+ oxidation states) is in a solid solution with bismuth in the molybdate scheelite structure.

Table 4. Comparison of cerium and lanthanum as promoters of bismuth molybdate for the selective ammoxidation of methanol to HCN [82].

Catalyst Composition	Reaction Temperature (°C)	% HCN Yield
$\text{K}_{0.1}\text{Bi}_4\text{Ce}_4\text{Mo}_{12}\text{O}_x$	410	75.2
$\text{K}_{0.1}\text{Bi}_4\text{La}_4\text{Mo}_{12}\text{O}_x$	410	55.9

3. Environmental Catalyst Applications

3.1. Combustion/Total Oxidation

As briefly mentioned above, catalysts for total oxidation typically function via a reaction mechanism involving the formation of surface-active oxygen species. The role of the catalyst is to create the sites conducive to the formation of these species [83]. In this role, cerium oxide has been found to be beneficial in creating such active sites due to the variable valance of cerium and the structural ability to accommodate oxygen vacancies. Cerium has been viewed for quite some time as an enabler for oxidation catalysis spanning a wide range of environmental remediation and renewable chemical applications [84,85].

3.1.1. CO Oxidation

The oxidation of CO to CO_2 has been one of the major thrusts of the development of catalysts for environmental protection. The focus is mostly on exhaust from transportation vehicles but application to stationary sources of CO has also been an area for catalyst development. In the case of catalysts for automobile exhaust application, technology development around supported complex multi-noble metals has been well developed both scientifically and commercially. In the most recent generations of automobile exhaust catalyst applications, cerium has become a well-established component of state-of-the-art

commercial catalytic converters because of its excellent thermal stability, redox stabilization of active oxygen species for oxidation, and ability to promote the high dispersion of the catalytically active and expensive noble metals. The application of cerium oxides to the design of automobile catalytic converters has been well documented and reviewed [86]. From a physical properties standpoint, the benefit of cerium oxide stems largely from its relatively higher resistance to sintering. With cerium oxide, usually in combination with the equally refractory zirconium oxide in solid solution, these physical properties translate into the maintenance of a high surface area (support sintering) and the high dispersion of the supported metals (metal sintering) compared to other oxide support materials, such as silica and alumina.

Much of the understanding of these catalysts has stemmed from studies of the main chemical target for the application, such as oxidation of CO, and a significant amount of research has been devoted to cerium oxide-containing catalysts to understand the fundamental surface and solid state mechanisms for cerium's role in the catalytic transformation to CO₂. The oxidation of CO over ceria-supported noble metal (Pt, Pd, Rh, Au, and Ag) catalysts is well known to proceed through lattice oxygens via the Mars–van Krevelen mechanism [87]. In the case of supported platinum catalysts after steam treatment, ceria support has been shown to be able not only to promote the high dispersion of the platinum and impart high thermal stability, but to also generate catalytically active sites through the stabilization of an atypical oxidation state for the supported metal, e.g., Pt²⁺. This significantly increases the catalytic activity and reduces the operating temperature of the catalyst by inducing the formation of highly active surface lattice oxygens for the oxidation of CO via a Mars–van Krevelen reaction mechanism [88].

3.1.2. Volatile Organic Compound (VOC) Oxidation

Catalysts for the remediation of low atmospheric concentrations of volatile organic compounds (VOC) at elevated temperature and pressure conditions as well as under ambient temperature conditions have increasingly incorporated cerium oxides because of the high redox activity of cerium and the excellent thermal and catalytic stability of ceria. The high temperature catalysts generally comprise noble metals, especially platinum, supported on ceria [89], while the low temperature catalyst variants are mixed oxides with ceria, although the supported noble metals platinum and gold with ceria can be effective under ambient conditions as well [90,91].

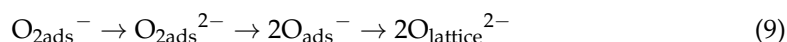
Formaldehyde has been a major focus of this process and catalyst development work because of its harmful effects on human health and strict workplace exposure regulations. Cerium has been incorporated along with other multivalent cations in a catalyst design strategy to augment the redox activity of the catalytically active species for the complete combustion to CO₂. Manganese oxides are among the most potent active catalyst constituents and the Ce³⁺/Ce⁴⁺ redox couple has been shown to work effectively to maintain the high catalytically active valence state of the Mn⁴⁺/Mn³⁺ redox couple via a proposed formation of an amorphous oxide solid solution of cerium and manganese [92,93]. Copper, as well, has been identified as an effective co-constituent with cerium for total oxidation processes because of its multivalent nature [94,95]. Interfacial effects are key to the catalysis as manganese and copper do not form continuous solid solutions with ceria and, thus, the dispersion of the manganese and copper on ceria is also critical. The ceria surface/interface typically contains neighboring Ce³⁺ and Ce⁴⁺ lattice sites. The catalytic site for oxidation is viewed as being at the interface of the binary oxide where partial metal lattice substitution is observed by Raman spectroscopy. This creates a so-called asymmetric oxygen vacancy site (ASO_v) by the substitution of Cu⁺ for Ce⁴⁺, which in turn is the active site for gaseous oxygen reduction to create the active oxygen-containing site for oxidation [96], as depicted in Equation (8).



In addition to formaldehyde and CO oxidation, cerium oxide as a catalyst and/or catalyst support has been reported to be beneficial in the total oxidation of a wide range

of other VOC hazardous pollutants, including chlorohydrocarbons [97], ethylene oxide, peroxides, propane [98], acetaldehyde, acrolein, aromatic hydrocarbons [99] including by photooxidation [100], acrylonitrile [101,102], HCN [103], and soot/particulates from diesel engine exhaust. Preparation methods also have a significant impact on ceria-supported Pt for VOC oxidation with the use of a metal–organic framework (MOF) as a precursor material in the synthesis resulting in a Pt/CeO₂ catalyst with enhanced Pt dispersion and higher turnover frequencies for toluene oxidation [104]. The loading of Pt on the ceria support is also a critical catalyst design parameter. Taking advantage of the strong Pt metal interaction with the ceria support, the metal loading can be optimized to maximize the catalytically active platinum species. Low loading results in the high dispersion of Pt metal, while very high loading results in the formation of less optimal metal clusters. An intermediate level optimizes the distance between Pt clusters and produces oxidized platinum clusters that are the key active sites for total oxidation. Maximizing these oxidized platinum active sites results in significantly reducing the light-off temperature for the reaction [105].

In summary, it is well established that the oxidation of VOC on cerium-containing catalysts proceeds by the reaction of the adsorbed organic molecule with lattice oxygens according to the Mars–van Krevelen mechanism. This mechanism results in the reduction of Ce⁴⁺ to Ce³⁺ during the surface oxidation reaction. The Ce³⁺ then serves as the site for gaseous O₂ reduction according to Equation (9) [106].



3.1.3. Soot and Particulate Oxidation—Diesel Engine Exhaust Emission Control

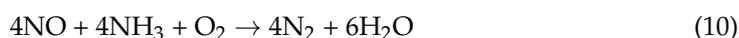
The abatement of particulates and soot from diesel engine exhaust is an area of catalyst technology where cerium is uniquely suited [107]. Ceria has been shown to be a highly effective catalyst constituent for combustion of diesel particulate emissions both as a support for noble metals [108] and as a mixed oxide [109,110] as is well-established and practiced commercially as an oxide solid solution with zirconium [111]. In addition, ceria can form continuous solid solutions with altrivalent cations, such as Pr³⁺ [112]. In the latter case, the fluorite structure of ceria forms a solid solution having the composition of Ce_xPr_{1-x}O_{2-δ} for 0.3 < x < 1. A similar strategy has been used with oxide solid solutions containing Ce, Pr, and Zr, wherein the presence of both Pr³⁺ and Pr⁴⁺ were observed [113]. This, combined with the multivalence of cerium and praseodymium, produces structural oxygen vacancies that can be accurately tuned by the presence of praseodymium to promote lattice oxygen mobility within the framework of the Mars–van Krevelen mechanism. The practical advantage of mixed-metal oxide catalysts compared to supported noble metal catalysts is their lower catalyst cost and improved thermal stability because of reduced sintering and catalyst deactivation. The use of oxide solid solutions offers a powerful catalyst design strategy to tailor the chemical and catalytic properties of the cations that occupy the same crystallographic site in the structure to a fine degree. This, in turn, provides a way to modify the nature of the active sites of the catalyst, and especially, the type and activity of the surface lattice oxygen species within the framework of the Mars–van Krevelen oxidation mechanism. For example, the adjustments of the relative amounts of the elemental constituents having different electronegativities for the La_{1-y}Ce_yCo_{1-x}Fe_xO₃ perovskite solid solution, as well as incorporating the two redox active cations cerium and iron in the same single-phase structure, directly controls the amount of the temperature-programmed desorption-measured β-O₂ responsible for the oxidation reaction [114].

An alternative approach to using solid cerium-containing materials in exhaust emission catalysts is the incorporation of the cerium catalyst as diesel fuel additive. The new technology has spawned several commercial fuel additive products, most notably Envirox™ [115,116] and one developed by Cerion™ [117], which consist of a nano-sized colloidal dispersion of ceria. The addition of nano-sized ceria to diesel fuel results in material reductions in the emission rates of CO, formaldehyde, acetaldehyde, and acrolein. Equally significant is the reduction in the emission of particulate soot. This remediation of

diesel emissions is a direct result of the catalytic redox activity of ceria to reduce the ignition temperature for the combustion of the carbon-containing compounds and particulates in the exhaust gas. The technology for preparing these nano-sized cerium dispersions is largely proprietary [118,119]. Nevertheless, the science relies on the well-established ability of cerium to form chelates with known organic complexing and dispersion agents, especially with citrates and tartrates [120,121].

3.2. NO_x Remediation

The selective catalytic reduction (SCR) of NO_x (nitrogen oxides, mostly NO, NO_2 and N_2O) is fundamentally a redox reaction that is generally catalyzed by mixed metal oxides that comprise elements capable of multiple oxidation states and that promote high lattice oxygen mobility. The SCR of NO in the presence of excess oxygen according to Equation (10) proceeds via a combination of Eley–Rideal and Mars–van Krevelen catalytic mechanisms [122,123].



The process is widely practiced industrially both at stationary (coal and natural gas-fueled power plants) and mobile (diesel-fueled vehicles) sources [124,125]. The most effective catalysts contain vanadium oxide (V_2O_5) with vanadium in the 5+ oxidation as the catalytically active surface moiety. The vanadium oxide is typically supported on TiO_2 with various other elements added to promote the reaction mechanism, including cerium [126]. The reaction pathway proceeds by the pre-adsorption of ammonia on a V^{5+} active site followed by reaction with gas phase NO in the rate determining step (Eley–Rideal). The resulting surface complex then decomposes and desorbs as N_2 and water that incorporates lattice oxygen from the vanadium oxide in the process (Mars–van Krevelen). The reduced V^{4+} is reoxidized to V^{5+} by the reduction of O_2 to lattice oxygen (Mars–van Krevelen).

The introduction of cerium into the vanadium oxide-based catalyst provides multiple enhancements to the operative mechanisms [127]. The most notable is the ability of the $\text{Ce}^{3+}/\text{Ce}^{4+}$ redox couple to stabilize vanadium, when present at the structural or interfacial vicinity of cerium, in its most active oxidation state of 5+ for the SCR reaction. This is evidenced, in part, by an enrichment of Ce^{3+} on the surface of CeO_2 -containing catalysts [128]. Numerous kinetic, computational, and characterization studies have supported this critical role for cerium in vanadium-containing SCR catalysts [129]. Cerium's catalytic role is driven by the availability of the cerium 4f state to accept electrons from reduced, V^{4+} , vanadium [130]. Cerium also promotes vanadium oxide-based SCR catalysts by creating additional acidic sites on the CeO_2 and/or CeVO_4 phases present in the catalyst. The acidic sites are active for ammonia adsorption and the rate determining step of the reaction of adsorbed ammonia (on either a Brønsted or Lewis acid site) with NO from the gas phase [131,132]. The method of catalyst preparation and incorporation of cerium into the catalyst was also shown to greatly affect cerium promotion [133] with the following order found for efficacy: hydrothermal treatment > sol–gel > co-precipitation > impregnation > mechanical mixing [134]. This order was attributed to maximizing the interaction of the catalyst components to enhance overall surface and lattice oxygen mobility as well as creating the surface acid sites necessary for the adsorption of the reactants.

The replacement of vanadium with manganese [135–140] or copper [141] as the active component for SCR of NO_x has received increasing attention because of the potential to function under lower temperature conditions than vanadium, which is a distinct economic process advantage. Here, cerium oxide has been shown to provide the same tangible benefits observed with vanadium oxide-based catalyst systems.

4. Bio-Based and Renewable Chemical Applications

4.1. General

Cerium has developed a unique niche as an impactful constituent of catalysts for the conversion of bio-based feedstocks to chemicals and fuels. In many bio-based conversion processes cerium oxide has been shown to be a powerful support material interacting

synergistically with several catalytic metals, notably platinum and gold. The origin of this catalytic benefit has been found to be severalfold: the redox behavior of cerium and its ability to stabilize a variety of active oxygen species important for the catalytic process, the structure sensitivity of cerium and specific crystal phases of cerium oxide in stabilizing the optimal configuration for the supported metal, and the resulting defect structures of cerium oxides that arise as a result of its multiple valency and generation of oxygen vacancies in the structure which promote a high dispersion of the supported metal up to single atom isolation. Additionally, the catalyst preparation chemistry for supporting the metal on cerium oxide has been found to play an additional role in realizing a synergistic metal-support interaction [142].

4.2. Select Bio-Based Catalytic Processes

One example of the investigation of cerium as a catalyst constituent in the conversion of a bio-based feedstock is the valorization of glycerol. Glycerol has been a frequent choice as a bio-based feedstock for chemical manufacture because it is a byproduct of biodiesel manufacture and, thus, is viewed as being representative of a low-cost and abundant renewable feedstock. Glycerol has been identified as a bio-based platform chemical with the potential to serve as a feedstock for a wide range of valuable chemical monomers, for example, acrolein for acrylic acid manufacture (piloted but not commercialized [143]), 1,2 propanediol (commercialized by ADM [144]), and hydroxyacetone (actively researched). The ability to prepare nanostructures of CeO_2 in a range of morphologies (nanorods, nanocubes, and nanooctahedra) has afforded the study of structure sensitivity of ceria catalysts [145]. This has allowed for the attribution of specific catalytic functions for glycerol valorization to each of the typically exposed ceria crystal faces: (100) favors glycerol dehydration to acrolein, and (110) and (111) favor hydroxyacetone and 1,2 propanediol formation from glycerol [146].

Among other platform chemical processes identified as viable research and development targets for commercial replacement with a bio-based chemical process is the selective oxidation of glucose to gluconic acid and glucaric acid [147]. For glucose oxidation, supported gold catalysts have been identified as uniquely active and selective for producing gluconic acid from glucose [148,149]. More specifically, ceria has found a unique niche in this space by being an especially effective support for gold as a catalyst for glucose oxidation. Again, structure sensitivity plays a role in the catalytic behavior of ceria [150]. Another sustainable platform chemical target that has been explored using a $\text{MnO}_x/\text{CeO}_2$ catalyst is 2,5-furandicarboxylic acid (FDCA) by the selective oxidation of 5-hydroxymethylfurfural, which can be readily produced from bio-based sources including fructose-containing sugars. Cerium oxide-containing catalysts have been reported to be effective for this oxidation reaction [151]. FDCA is viewed as the basic monomer for a new family of furanic polymers and polyesters that can replace polyethylene terephthalate (PET), especially in beverage bottles, and impart improved gas barrier properties. Cerium again promotes catalytic activity and enhances FDCA yield in an active and selective $\text{MnO}_x/\text{CeO}_2$ catalyst via its redox activity, which maintains the catalytically active surface site in the Mn^{4+} oxidation state. The enrichment of Ce^{3+} promotes reoxidation and lattice oxygen transfer on the catalyst surface [152]. This is the same promotion mechanism noted above for VO_x/CeO_2 redox catalysts.

A significant hurdle to the incorporation of cerium into many bio-conversion catalysts is that many of these processes are required to operate in aqueous environments, which augurs the possibility of deactivation by solubilization of cerium. The relatively basic cerium oxide accentuates the problem when the aqueous process produces acidic products as in the case of gluconic and glucaric acids, and/or is conducted under base-free conditions, which is in many cases preferable because of easier downstream separation and purification. Approaches to ameliorate the solubility of cerium in oxide catalysts have focused on preparation methods, especially those that can produce nano-structures of cerium oxide

that are relatively more stable under the relatively mild reaction conditions required for a bio-based process.

5. Underpinnings for Cerium Oxide Catalysts

5.1. Chemical and Physical Properties of Cerium Oxides Relevant to Catalysis

Cerium redox chemistry and ceria oxygen storage capacity are at the heart of the inroads cerium has made as a key catalyst constituent, especially for oxidative chemical transformations. The $4f^15d^26s^2$ electron configuration of cerium and the accessibility of the f electron state allows for the existence of both the Ce^{3+} or Ce^{4+} oxidation states. A favorable redox potential, in turn, imparts facile redox activity at elevated temperatures (>600 K) that has made cerium oxides successful catalysts in oxidation reactions, fuel cells, oxygen pumps, solid-state electrolytes, and ionic conductors [153]. Numerous studies have been undertaken to understand the ability of cerium oxide to serve as a powerful and unique catalyst promoter for a wide range of chemical transformations described herein. These characterization studies generally have focused on two aspects of cerium oxide chemistry—its solid-state structural characteristics and its multivalent/redox properties. Cerium can impact the behavior of a catalytically active oxide phase either by (i) direct incorporation into the crystallographic structure of the active oxide phase or by (ii) close proximity and maximal contact (i.e., interfacial effect) with the catalytically active phase. Both have been shown to be effective mechanisms by which the redox properties of cerium can be integrated into the catalytic cycle driven by the components of the active phase.

The direct incorporation of cerium in an oxide crystal structure (i.e., solid solution) has been extensively studied for two crystal structure types—fluorite-related and scheelite-related—and both are well-established in use in catalytic applications. The first is the $Ce_xZr_{1-x}O_2$ that forms the basis for the commercial automobile exhaust catalyst system described above. The formation of this solid solution is not surprising given the small difference in the ionic radii of Ce^{4+} and Zr^{4+} —0.097 nm for the former and 0.084 nm for the latter. CeO_2 crystallizes in the cubic fluorite structure while ZrO_2 is polymorphic, having a monoclinic structure up to 1443 K, a tetragonal structure between 1443 K and 2643 K, and a cubic fluorite structure between 2643 K and its melting point at 2988 K. At temperatures below 1273 K (typically the maximum operating and/or catalyst synthesis temperature), the $Ce_xZr_{1-x}O_2$ solid solution can be viewed as generally consisting of equilibrium mixtures of monoclinic $Ce_{0.15}Zr_{0.88}O_2$ and cubic $Ce_{0.84}Zr_{0.16}O_2$. However, detailed characterization studies point to the presence of two non-equilibrium tetragonal structures as well within this composition range [154]. Irrespective of the details of the phase diagram and phase composition under synthesis or reaction conditions, the key chemical aspect as it is related to catalytic behavior is that the solid solution provides a structural framework within which the redox activity of cerium can operate. In the case of CeO_2/ZrO_2 solid solutions, regardless of crystal structure, cerium's catalytic role is to provide a high oxygen storage capacity and facile movement of lattice and surface oxygen. Zirconium is not, per se, catalytically active but instead provides the thermal stability to mitigate sintering (loss of surface area) under the high temperature (600 K to 1300 K) reaction conditions that the catalyst system needs to function.

A different situation with respect to catalytic roles occurs with scheelite solid solutions containing cerium as catalysts for selective oxidation reactions. Bismuth–cerium–molybdenum-oxide exists as a defect scheelite structure [155,156] and forms a continuous solid solution across the composition range $Bi_xCe_{2-x}Mo_3O_{12}$ with $0 \leq x \leq 2$, where denotes a structural cation vacancy within the representative $CaWO_4$ scheelite structure [157]. The partial phase diagram (see Figure 5) consists of two bismuth–cerium–molybdenum-oxide solid solutions: One solid solution consists of cerium dissolved in the α - $Bi_2Mo_3O_{12}$ structure for x greater than about 1.8. The second solid solution has bismuth dissolved in the cerium molybdate structure when x is less than about one. The enhanced catalytic activity of the cerium-containing formulations for the selective ammoxidation of propene to acrylonitrile is attributed to the presence of the Ce^{3+}/Ce^{4+} redox couple in the presence of the

catalytically active Bi^{3+} that is responsible for rate determining α -H abstraction of adsorbed propene. The incorporation of the cerium redox couple into both the surface and the bulk structures facilitates lattice oxygen transfer to the bismuth- and molybdenum-containing active site as required by the operative Mars–van Krevelen mechanism for selective propene ammoxidation.

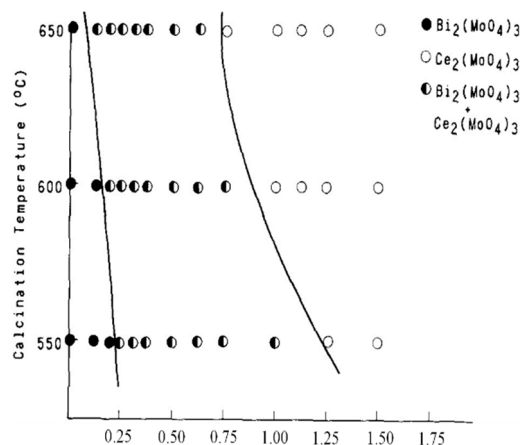


Figure 5. Partial phase diagram of $\text{Bi}_{1-x}\text{Ce}_x\text{Mo}_3\text{O}_{12}$ where x is shown on the x -axis. Source with permission [34].

Thus, in contrast to the case of the $\text{Ce}_x\text{Zr}_{1-x}\text{O}_2$ solid solution where the zirconium serves as a structural host for the catalytically functioning cerium, the $\text{Bi}_x\text{Ce}_{2-x}\text{Mo}_3\text{O}_{12}$ solid solution incorporates the redox active promoter, cerium, into the same structural phase with the catalytically active components, bismuth and molybdenum. The further refinement of the structure by X-ray and neutron diffraction analyses along with Rietveld data analysis shows that both of the bismuth–cerium–molybdenum-oxide solid solutions are not conventional with the random distribution of bismuth and cerium in the large cation site of the scheelite structure. Instead, Ce^{3+} preferentially occupies one of the three crystallographic sites, which puts it in direct proximity to the catalytically active Bi^{3+} that is responsible for the rate determining step of hydrogen abstraction in the selective (amm)oxidation of propene [158]. This work has shown the importance of the site occupancy and oxygen coordination of the cerium in this defect scheelite structure in creating a highly effective active site for the mechanistic steps of activation, chemical transformation, and reoxidation in the catalytic cycle.

The role of interfacial effects are manifest when ceria is used as a support for a catalytically active metal. In the case of the copper/ceria catalysts used for methanol synthesis from CO_2 for example, the interface between the copper and ceria contains the sites for for CO_2 activation [159]. Maximizing the interfacial contact by synthesizing nano-sized ceria as the support increases catalytic activity by increasing the number of metal active sites. In the case of Pt/CeO_2 , the use of nano-structure ceria supports in contact with nano-sized Pt enhances the electron transfer from Pt to CeO_2 and the transfer of activated oxygen from CeO_2 to Pt [160]. This enhanced transfer only occurs for the nanoparticle ceria and Pt that are in direct contact. Ceria support, thus, plays a powerful role in controlling the catalytic behavior of the supported metal as a result of these interfacial effects.

Other studies have confirmed that the most catalytically active sites on ceria supported metal catalysts reside at the point of contact of the metal, support and the reaction atmosphere irrespective of the geometries of the metal or support [161]. Smaller metal particles provide the highest activity due to larger surface-to-volume ratios and thus increased boundary length between the metal and the ceria support. The correlation of calculations of metal/ceria interfacial contact with turnover frequency for CO oxidation on ceria-supported metal catalysts implies the active site location is at the interface between

photocatalysis, energy storage, and fuel cells. High-entropy single-phase solid solutions generally consist of metal alloys [165] or multi-metal oxides [166], borides, carbides, nitrides, sulfides, or silicides in which five or more elemental constituents in equimolar or near equimolar concentrations coexist within a single crystallographic structure. They have been found to provide new and improved chemical, mechanical, thermal, and electronic properties in a wide range of material applications, including electronics, ceramics, energy storage devices, magnets, and catalysts [167]. They are generally metastable compounds in that they require quenching after high-temperature synthesis to maintain a single-phase structure. In the case of catalyst applications, high-entropy solid solutions confer unique effects on a material's properties by bringing together in a single structural environment a spectrum of elements, each with its own specific mechanistic function for the catalyzed reaction. They also create localized defect structures, such as oxygen vacancies, lattice distortions, and electronic interactions between disparate elements that either serve as the active site for the catalysis or augment a critical property, such as oxygen transfer and mobility in the lattice. The redox activity and defect chemistry of cerium makes it well suited for designing catalysts for the oxidative chemical transformations that were described in this review. More specifically, cerium has proven to be a key component of many new material applications, most notably within the context of scheelite-structured solid solutions [168]. The multiple valency of cerium also provides it the advantage of being able to control the relative content of Ce^{4+} and Ce^{3+} by modifying the atmosphere (oxygen-containing or oxygen-free) during the high temperature synthesis of the material. For example, the high-entropy scheelite solid solution $(\text{Ca}_{0.5}\text{Ce}_{0.5})(\text{Nb}_{0.25}\text{Ta}_{0.25}\text{Mo}_{0.25}\text{W}_{0.25})\text{O}_4$ can combine multiple oxidation states for cerium, defects in the form of oxygen and cation vacancies, and distinct lattice distortions as a result of the random distribution of cations of varying size in the same crystallographic site of a single crystallographic structure, as shown in Figure 7.

The growth in the development and application of cerium-containing materials since about 1980 has truly been remarkable. Cerium has been applied to many of the major fields of fundamental and applied catalysis and continues to be exploited for its redox and defect structural properties in many emerging technology applications as well, including CO_2 conversion [169], advanced fuel cell technologies [170], biomimetic catalysis [171], and the manufacture of sustainable aviation fuels [172,173]. The application of cerium oxide to catalysis, which started as a redox promoter and then as an "inert" support for metal catalysts, has grown into a dynamic field of rational catalyst design based on the increased understanding of cerium's unique redox properties, structural versatility, and agency as a catalyst constituent.

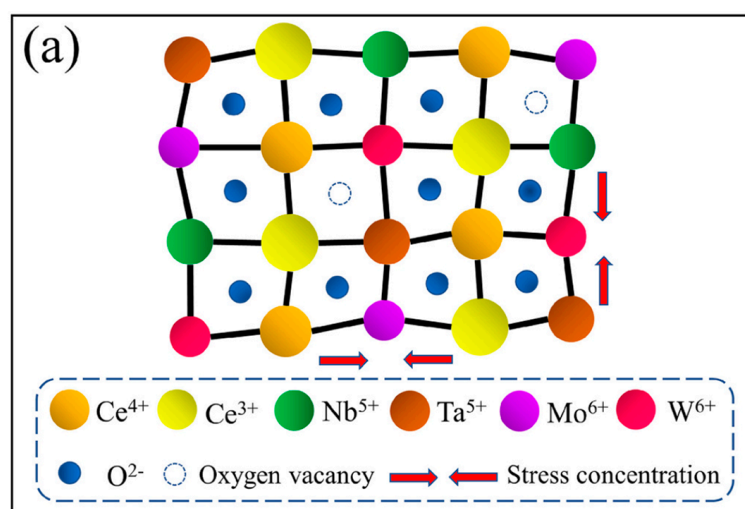


Figure 7. Cont.

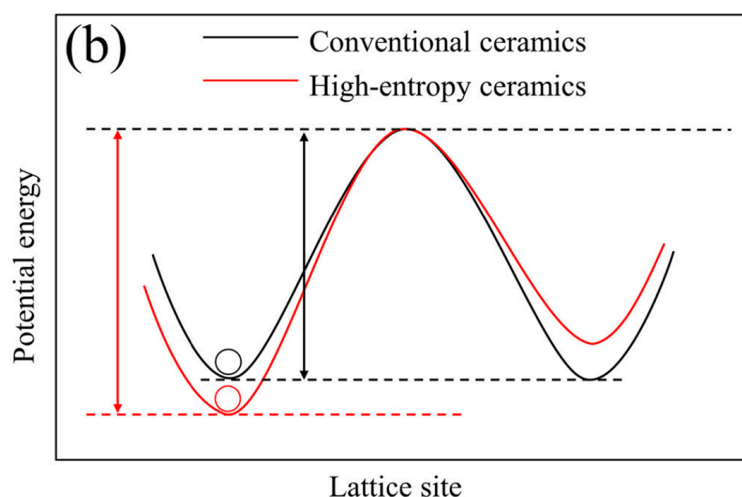


Figure 7. (a) Schematic diagram of lattice distortion effect in $(\text{Ca}_{0.5}\text{Ce}_{0.5})(\text{Nb}_{0.25}\text{Ta}_{0.25}\text{Mo}_{0.25}\text{W}_{0.25})\text{O}_4$ high-entropy ceramics; (b) potential energy of ions in high-entropy and conventional ceramics. Source with permission: [168].

Funding: This research received no external funding.

Data Availability Statement: Not applicable.

Acknowledgments: The author thanks his many colleagues at INEOS for their many contributions to the fundamental and applied research of cerium-containing oxide catalysts for the manufacture of acrylonitrile from propene that is discussed herein. The author wishes to thank Linda Brazdil for expert review of the manuscript and to the University of Houston for access to library resources.

Conflicts of Interest: The author declares no conflict of interest.

References

- Grasselli, R.K.; Callahan, J.L. Structure-catalytic efficiency relations in uranium-antimony oxide acrylonitrile synthesis catalysts. *J. Catal.* **1969**, *14*, 93–103. [\[CrossRef\]](#)
- Grasselli, R.K.; Suresh, D.D. Aspects of structure and activity in uranium-antimony oxide acrylonitrile catalysts. *J. Catal.* **1972**, *25*, 273. [\[CrossRef\]](#)
- Suresh, D.D.; Grasselli, R.K. Uranium Antimonate Catalysts. U.S. Patent 4317747, 2 March 1982.
- Montini, T.; Melchionna, M.; Monai, M.; Fornasiero, P. Fundamentals and Catalytic Applications of CeO₂-Based Materials. *Chem. Rev.* **2016**, *116*, 5987–6041. [\[CrossRef\]](#) [\[PubMed\]](#)
- He, J.-J.; Wang, C.-X.; Zheng, T.-T.; Zhao, Y.-K. Thermally Induced Deactivation and the Corresponding Strategies for Improving Durability in Automotive Three-Way Catalysts. *Johns. Matthey Technol. Rev.* **2016**, *60*, 196–203. [\[CrossRef\]](#)
- Brazdil, J.F.; Teller, R.G.; Grasselli, R.K.; Kostiner, E. Structural and thermodynamic basis for catalytic behavior of bismuth-cerium molybdate selective oxidation catalysts. *ACS Symp. Ser.* **1985**, *279*, 57–74. [\[CrossRef\]](#)
- Valange, S.; Védrine, J.C. General and Prospective Views on Oxidation Reactions in Heterogeneous Catalysis. *Catalysts* **2018**, *8*, 483. [\[CrossRef\]](#)
- Eley, D.D.; Rideal, E.K. Parahydrogen conversion on tungsten. *Nature* **1940**, *146*, 401. [\[CrossRef\]](#)
- Mars, P.; van Krevelen, D.W. Oxidations carried out by means of vanadium oxide catalysts. *Chem. Eng. Sci.* **1954**, *3*, 41–59. [\[CrossRef\]](#)
- Kawano, T.; Takahashi, Y.; Fukumoto, N. Catalyst for Producing Unsaturated Aldehyde and/or Unsaturated Carboxylic Acid and Method for Producing Unsaturated Aldehyde and/or Unsaturated Carboxylic Acid Using Catalyst. WO2012036038, 22 March 2012.
- Dolhyj, S.R.; Milberger, E.C. Acrylic Acid or Methacrylic Acid. DE 2,448,804, 30 April 1975.
- Yunoki, H.; Tanimoto, M.; Nakamura, D. Manufacture of Acrylic Acid by Vapor-Phase Catalytic Oxidation of Acrolein. EP 1,055,662, 29 November 2000.
- Aykan, K. Reduction of Bi₂O₃·MoO₃ catalyst during the ammoxidation of propylene in the absence of gaseous oxygen. *J. Catal.* **1968**, *12*, 281–290. [\[CrossRef\]](#)
- Van den Elzen, A.F.; Rieck, G.D. An outline of the crystal-structure of Bi₂Mo₂O₉. *Mater. Res. Bull.* **1975**, *10*, 1163–1168. [\[CrossRef\]](#)
- Teller, R.G.; Brazdil, J.F.; Grasselli, R.K. The structure of γ -bismuth molybdate, Bi₂MoO₆, by powder neutron diffraction. *Acta Crystallogr. Sect. C Cryst. Struct. Commun.* **1984**, *C40*, 2001–2005. [\[CrossRef\]](#)
- Sennewald, K.; Vogt, W.; Kandler, J.; Sommerfeld, R.; Sorbe, G. Process for Preparing Unsaturated Nitriles. U.S. Patent 3226422, 28 December 1965.

17. Sennewald, K.; Vogt, W.; Kandler, J.; Sommerfeld, R.; Sorbe, G. Process for Preparing Acrylonitrile. U.S. Patent Re27718, 7 August 1973.
18. Yamaguchi, G.; Takenaka, S. Process for the Oxidation of Olefins to Aldehydes and Acids. U.S. Patent 3454630, 8 July 1969.
19. Grasselli, R.K.; Miller, A.F.; Hardman, H.F. Catalysts and Process for the Ammoxidation of Olefins. U.S. Patent 4192776, 11 March 1980.
20. Sugiyama, S.; Miyake, M.; Yoshida, M.; Nakao, Y.; Shimoda, N.; Katoh, M. Effect of cerium addition to bismuth-molybdenum complex oxide catalyst for partial oxidation of propylene to acrolein. *J. Jpn. Pet. Inst.* **2020**, *63*, 267–273. [[CrossRef](#)]
21. Yang, H.; Fan, Y.; Wu, J.; Chen, Y. Structure and properties of BiCeVMoO mixed metal oxides catalysts for selective oxidation of propane. *J. Mol. Catal. A: Chem.* **2005**, *227*, 279–283. [[CrossRef](#)]
22. Zhang, X.; Wan, H.-L.; Weng, W.-Z.; Yi, X.-D. Selective Oxidation of Propane to Acrolein over Ce-Doped Ag-Mo-P-O Catalysts: Influence of Ce Promoter. *Catal. Lett.* **2003**, *87*, 229–234. [[CrossRef](#)]
23. Zhang, X.; Wan, H.; Weng, W. Reaction pathways for selective oxidation of propane to acrolein over Ce-Ag-Mo-P-O catalysts. *Appl. Catal. A Gen.* **2009**, *353*, 24–31. [[CrossRef](#)]
24. Fischer, A.; Burkhardt, W.; Weckbecker, C.; Huthmacher, K.; Wilz, F. Mixed Oxide Catalysts for the Catalytic Gas-Phase Oxidation of Olefins. WO2007042369, 19 April 2007.
25. Brazdil, J.F. Acrylonitrile. In *Ullmann's Encyclopedia of Industrial Chemistry*; Wiley-VCH: Weinheim, Germany, 2012. [[CrossRef](#)]
26. Idol, J.D., Jr. Acrylonitrile. U.S. Patent 2904580, 15 September 1959.
27. Veatch, F.; Callahan, J.L.; Milberger, E.C.; Foreman, R.W. Catalytic Oxidation of Propylene to Acrolein. In Proceedings of the 2nd International Congress on Catalysis, Paris, France, 4–8 July 1960; Volume 2, p. 2647.
28. Giordano, N.; Bart, J.C.J. Structure-activity relations in cerium molybdenum tellurium oxide acrylonitrile catalysts. *Geterog. Katal.* **1979**, *4 Pt 2*, 27–32.
29. Bart, J.C.J.; Giordano, N. Structure of the cerium-molybdenum-tellurium oxide acrylonitrile catalyst. *Ind. Eng. Chem. Prod. Res. Dev.* **1984**, *23*, 56–62. [[CrossRef](#)]
30. Bart, J.C.J.; Giordano, N. Structure and activity of tellurium-molybdenum oxide acrylonitrile catalysts. *J. Catal.* **1980**, *64*, 356. [[CrossRef](#)]
31. Bart, J.C.J.; Giordano, N. Structure and activity of tellurium-cerium oxide acrylonitrile catalysts. *J. Catal.* **1982**, *75*, 134–139. [[CrossRef](#)]
32. Bart, J.C.J.; Giordano, N.; Forzatti, P. Phase relationships in the cerium-molybdenum-tellurium oxide system. *ACS Symp. Ser.* **1985**, *279*, 89–101. [[CrossRef](#)]
33. Giordano, N.; Bart, J.C.J. Mechanism of ammoxidation of propene over cerium-doped bismuth molybdate catalysts. *Recl. Trav. Chim. Pays-Bas* **1975**, *94*, 28–30. [[CrossRef](#)]
34. Brazdil, J.F.; Grasselli, R.K. Relationship between solid state structure and catalytic activity of rare earth and bismuth-containing molybdate ammoxidation catalysts. *J. Catal.* **1983**, *79*, 104–117. [[CrossRef](#)]
35. Brazdil, J.F.; Glaeser, L.C.; Grasselli, R.K. Role of interfacial phenomena in the catalytic behavior of multiphase selective ammoxidation catalysts. *J. Phys. Chem.* **1983**, *87*, 5485–5491. [[CrossRef](#)]
36. Xu, H.; Liu, J. Catalytic properties of Ce containing composite oxide for ammoxidation of propylene. In *Xinshiji De Cuihau Kexue Yu Jishu, Quanguo Cuihuaxue Jihuiyi Lunwenji, 10th, Zhangjiajie, China, 15–19 October 2000*; Shanxi Kexue Jishu Chubanshe: Taiyuan, China, 2000; p. 245.
37. Xu, H.; Liu, J. Catalytic behavior of cerium-containing multicomponent oxide for ammoxidation of propylene. *Huaxue Shijie* **2002**, *43*, 401–403.
38. Aoki, K.; Honda, M.; Dozono, T.; Katsumata, T. Catalyst Composition. U.S. Patent 4443556, 17 April 1984.
39. Suresh, D.D.; Friedrich, M.S.; Seely, M.J. Catalyst for Process for the Manufacture of Acrylonitrile and Methacrylonitrile. U.S. Patent 5093299, 3 March 1992.
40. Suresh, D.D.; Friedrich, M.S.; Seely, M.J. Catalyst for the Manufacture of Acrylonitrile and Methacrylonitrile. U.S. Patent 5212137, 18 May 1993.
41. Midorikawa, H.; Someya, K.; Aoki, K.; Nagano, O. Ammoxidation Catalyst Composition, and Process for Producing Acrylonitrile or Methacrylonitrile Using the Same. U.S. Patent 5658842, 19 August 1997.
42. Papparizos, C.; Jevne, S.C.; Seely, M.J. Catalyst for the Manufacture of Acrylonitrile. U.S. Patent 7071140, 4 July 2006.
43. Papparizos, C.; Jevne, S.C.; Seely, M.J. Catalyst for the Manufacture of Acrylonitrile. U.S. Patent 7348291, 25 March 2008.
44. Zheng, Y.; Yang, T.; Yu, Z.; Zhao, J.; Cai, H.; Zhao, Q. Structure of active phases of cerium-containing multicomponent oxide and its catalytic behavior for ammoxidation of propylene. *Yingyong Huaxue* **1988**, *5*, 13–17.
45. Brazdil, J.F.; Suresh, D.D.; Grasselli, R.K. Preparation of Acrylonitrile from Propylene, Oxygen, and Ammonia in the Presence of an Alkali Metal Promoted Bismuth, Cerium, Molybdenum, Tungsten Catalyst. U.S. Patent 4746753, 24 May 1988.
46. Brazdil, J.F.; Lin, S.Y. Ammoxidation Catalysts Containing Samarium. U.S. Patent Application 20170114007, 27 April 2017.
47. Yoshida, J.; Yamaguchi, T. Oxide Catalyst and Method for Producing the Same, and Methods for Producing Unsaturated Aldehyde, Diolefin, and Unsaturated Nitrile. U.S. Patent 9364817, 14 June 2016.
48. Brazdil, J.F. Designing multifunctionality into single phase and multiphase metal-oxide-selective propylene ammoxidation catalysts. *Catalysts* **2018**, *8*, 103. [[CrossRef](#)]
49. Brazdil, J.F.; Toft, M.A.; McKenna, S.T. Mixed Metal Oxide Catalysts. U.S. Patent 9433929, 6 September 2016.
50. Brazdil, J.F.; Toft, M.A. Mixed Metal Oxide Ammoxidation Catalysts. U.S. Patent Application 20160175817, 23 June 2016.

51. Fukuzawa, A.; Kaneta, M. Fluid Bed Ammoxidation Reaction Catalyst Comprising Silica and Metal Oxide, and Production Method of Acrylonitrile Using Same. WO2017130906, 3 August 2017.
52. Iitsuka, C.; Fukuzawa, A. Catalyst, Method for Manufacturing Catalyst, and Method for Manufacturing Acrylonitrile. WO2020213362, 22 October 2020.
53. Ushikubo, T.; Oshima, K.; Kayo, A.; Umezawa, T.; Kiyono, K.-I.; Sawaki, I.; Nakamura, H. Molybdenum Oxide Ammoxidation Catalyst for the Production of Nitriles. U.S. Patent 5472925, 5 December 1995.
54. Wang, G.; Guo, Y.; Lu, G. Promotional effect of cerium on Mo-V-Te-Nb mixed oxide catalyst for ammoxidation of propane to acrylonitrile. *Fuel Process. Technol.* **2015**, *130*, 71–77. [CrossRef]
55. Grasselli, R.K. Selectivity issues in (amm)oxidation catalysis. *Catal. Today* **2005**, *99*, 23–31. [CrossRef]
56. Grasselli, R.K.; Buttrey, D.J.; Burrington, J.D.; Andersson, A.; Holmberg, J.; Ueda, W.; Kubo, J.; Lugmair, C.G.; Volpe, A.F. Active centers, catalytic behavior, symbiosis and redox properties of MoV(Nb,Ta)TeO ammoxidation catalysts. *Top. Catal.* **2006**, *38*, 7–16. [CrossRef]
57. Grasselli, R.K.; Buttrey, D.J.; DeSanto, P.; Burrington, J.D.; Lugmair, C.G.; Volpe, A.F.; Weingand, T. Active centers in Mo-V-Nb-Te-Ox (amm)oxidation catalysts. *Catal. Today* **2004**, *91–92*, 251–258. [CrossRef]
58. Goddard, W.A., III; Mueller, J.E.; Chenoweth, K.; van Duin, A.C.T. ReaxFF Monte Carlo reactive dynamics: Application to resolving the partial occupations of the M1 phase of the MoVNbTeO catalyst. *Catal. Today* **2010**, *157*, 71–76. [CrossRef]
59. Cheng, M.-J.; Goddard, W.A., III. In Silico Design of Highly Selective Mo-V-Te-Nb-O Mixed Metal Oxide Catalysts for Ammoxidation and Oxidative Dehydrogenation of Propane and Ethane. *J. Am. Chem. Soc.* **2015**, *137*, 13224–13227. [CrossRef] [PubMed]
60. Sano, K.; Kaneko, K. Method for Purification of Acrylonitrile Manufactured by Catalytic Ammoxidation of Propane. JP2010222309, 10 July 2010.
61. Grand Opening Ceremony for AN and MMA Plants in Thailand. 2013. Available online: https://www.asahi-kasei.co.jp/asahi/en/news/2012/e130213_1.html (accessed on 18 May 2022).
62. Ishii, Y.; Okada, K. Oxide Catalyst, Production Method Therefor, and Unsaturated-Nitrile Production Method. WO2015133510, 11 September 2015.
63. Brazdil, J.F. The legacy and promise of heterogeneous selective oxidation and ammoxidation catalysis. *Catal. Today* **2021**, *363*, 55–59. [CrossRef]
64. Bej, S.K.; Rao, M.S. Selective oxidation of n-butane to maleic anhydride. 1. Optimization studies. *Ind. Eng. Chem. Res.* **1991**, *30*, 1819–1824. [CrossRef]
65. Bej, S.K.; Rao, M.S. Selective oxidation of n-butane to maleic anhydride: A comparative study between promoted and unpromoted VPO catalysts. *Appl. Catal. A Gen.* **1992**, *83*, 149–163. [CrossRef]
66. López Nieto, J.M.; Solsona, B.; Védrine, J.C. 5-Gas phase heterogeneous partial oxidation reactions. In *Metal Oxides in Heterogeneous Catalysis*; Elsevier: Amsterdam, The Netherlands, 2018; pp. 211–286.
67. Brazdil, J.F. Selective oxidation in industry: Applications of metal oxides in the petrochemical industry. In *Metal Oxides in Heterogeneous Catalysis*; Elsevier, B.V.: Amsterdam, The Netherlands, 2018; pp. 455–502.
68. Daniell, W.; Ponchel, A.; Kuba, S.; Anderle, F.; Weingand, T.; Gregory, D.H.; Knoezinger, H. Characterization and Catalytic Behavior of VOx-CeO₂ Catalysts for the Oxidative Dehydrogenation of Propane. *Top. Catal.* **2002**, *20*, 65–74. [CrossRef]
69. Yun, Y.S.; Lee, M.; Sung, J.; Yun, D.; Kim, T.Y.; Park, H.; Lee, K.R.; Song, C.K.; Kim, Y.; Lee, J.; et al. Promoting effect of cerium on MoVTeNb mixed oxide catalyst for oxidative dehydrogenation of ethane to ethylene. *Appl. Catal. B* **2018**, *237*, 554–562. [CrossRef]
70. Wan, C.; Cheng, D.-G.; Chen, F.; Zhan, X. The role of active phase in Ce modified BiMo catalysts for oxidative dehydrogenation of 1-butene. *Catal. Today* **2016**, *264*, 180–184. [CrossRef]
71. Martinez-Huerta, M.V.; Coronado, J.M.; Fernandez-Garcia, M.; Iglesias-Juez, A.; Deo, G.; Fierro, J.L.G.; Banares, M.A. Nature of the vanadia-ceria interface in V⁵⁺/CeO₂ catalysts and its relevance for the solid-state reaction toward CeVO₄ and catalytic properties. *J. Catal.* **2004**, *225*, 240–248. [CrossRef]
72. Park, S.M.; Jeon, S.W.; Kim, S.H. Formaldehyde Oxidation Over Manganese-Cerium-Aluminum Mixed Oxides Supported on Cordierite Monoliths at Low Temperatures. *Catal. Lett.* **2014**, *144*, 756–766. [CrossRef]
73. Feng, T.; Vohs, J.M. A TPD study of the partial oxidation of methanol to formaldehyde on CeO₂-supported vanadium oxide. *J. Catal.* **2004**, *221*, 619–629. [CrossRef]
74. Ganduglia-Pirovano, M.V.; Popa, C.; Sauer, J.; Abbott, H.; Uhl, A.; Baron, M.; Stacchiola, D.; Bondarchuk, O.; Shaikhutdinov, S.; Freund, H.-J. Role of Ceria in Oxidative Dehydrogenation on Supported Vanadia Catalysts. *J. Am. Chem. Soc.* **2010**, *132*, 2345–2349. [CrossRef]
75. Kropp, T.; Paier, J.; Sauer, J. Support Effect in Oxide Catalysis: Methanol Oxidation on Vanadia/Ceria. *J. Am. Chem. Soc.* **2014**, *136*, 14616–14625. [CrossRef] [PubMed]
76. Abbott, H.L.; Uhl, A.; Baron, M.; Lei, Y.; Meyer, R.J.; Stacchiola, D.J.; Bondarchuk, O.; Shaikhutdinov, S.; Freund, H.J. Relating methanol oxidation to the structure of ceria-supported vanadia monolayer catalysts. *J. Catal.* **2010**, *272*, 82–91. [CrossRef]
77. Vining, W.C.; Strunk, J.; Bell, A.T. Investigation of the structure and activity of VOx/CeO₂/SiO₂ catalysts for methanol oxidation to formaldehyde. *J. Catal.* **2012**, *285*, 160–167. [CrossRef]
78. Kropp, T.; Paier, J. Activity versus Selectivity of the Methanol Oxidation at Ceria Surfaces: A Comparative First-Principles Study. *J. Phys. Chem. C* **2015**, *119*, 23021–23031. [CrossRef]

79. Lustemberg, P.G.; Bosco, M.V.; Bonivardi, A.; Busnengo, H.F.; Ganduglia-Pirovano, M.V. Insights into the Nature of Formate Species in the Decomposition and Reaction of Methanol over Cerium Oxide Surfaces: A Combined Infrared Spectroscopy and Density Functional Theory Study. *J. Phys. Chem. C* **2015**, *119*, 21452–21464. [[CrossRef](#)]
80. Sutton, J.E.; Danielson, T.; Beste, A.; Savara, A. Below-Room-Temperature C–H Bond Breaking on an Inexpensive Metal Oxide: Methanol to Formaldehyde on CeO₂(111). *J. Phys. Chem. Lett.* **2017**, *8*, 5810–5814. [[CrossRef](#)]
81. Capdevila-Cortada, M.; García-Melchor, M.; López, N. Unraveling the structure sensitivity in methanol conversion on CeO₂: A DFT+U study. *J. Catal.* **2015**, *327*, 58–64. [[CrossRef](#)]
82. Brazdil, J.F., Jr.; Attig, T.G.; Grasselli, R.K. Ammoxidation of Methanol to Produce Hydrogen Cyanide. U.S. Patent 4485079, 27 November 1984.
83. Haber, J. Selective oxidations: Fundamentals of hydrocarbon oxidation. In *Handbook of Heterogeneous Catalysis*, 2nd ed.; Wiley-VCH: Weinheim, Germany, 2008; p. 3359.
84. Beckers, J.; Rothenberg, G. Sustainable selective oxidations using ceria-based materials. *Green Chem.* **2010**, *12*, 939–948. [[CrossRef](#)]
85. Arena, F. Multipurpose composite MnCeOx catalysts for environmental applications. *Catal. Sci. Technol.* **2014**, *4*, 1890–1898. [[CrossRef](#)]
86. Yoshida, H.; Koide, T.; Uemura, T.; Kuzuhara, Y.; Ohyama, J.; Machida, M. Ce-modified Rh Overlayer for a Three-Way Catalytic Converter with Oxygen Storage/Release Capability. *Catal. Today*, **2022**, in press. [[CrossRef](#)]
87. Wang, H.; Luo, S.; Zhang, M.; Liu, W.; Wu, X.; Liu, S. Roles of oxygen vacancy and Ox– in oxidation reactions over CeO₂ and Ag/CeO₂ nanorod model catalysts. *J. Catal.* **2018**, *368*, 365–378. [[CrossRef](#)]
88. Nie, L.; Mei, D.; Xiong, H.; Peng, B.; Ren, Z.; Hernandez Xavier Isidro, P.; DeLaRiva, A.; Wang, M.; Engelhard Mark, H.; Kovarik, L.; et al. Activation of surface lattice oxygen in single-atom Pt/CeO₂ for low-temperature CO oxidation. *Science* **2017**, *358*, 1419–1423. [[CrossRef](#)]
89. Salaev, M.A.; Salaeva, A.A.; Kharlamova, T.S.; Mamontov, G.V. Pt–CeO₂-based composites in environmental catalysis: A review. *Appl. Catal. B Environ.* **2021**, *295*, 120286. [[CrossRef](#)]
90. Wang, S.; Wang, Y.; Wang, F. Room temperature HCHO oxidation over the Pt/CeO₂ catalysts with different oxygen mobilities by changing ceria shapes. *Appl. Catal. A Gen.* **2022**, *630*, 118469. [[CrossRef](#)]
91. Gaňlová, J.; Topka, P. Gold and Ceria as Catalysts for VOC Abatement: A Review. *Catalysts* **2021**, *11*, 789. [[CrossRef](#)]
92. Huang, Q.; Lu, Y.; Si, H.; Yang, B.; Tao, T.; Zhao, Y.; Chen, M. Study of Complete Oxidation of Formaldehyde Over MnOx–CeO₂ Mixed Oxide Catalysts at Ambient Temperature. *Catal. Lett.* **2018**, *148*, 2880–2890. [[CrossRef](#)]
93. Guan, S.; Huang, Q.; Ma, J.; Li, W.; Ogunbiyi, A.T.; Zhou, Z.; Chen, K.; Zhang, Q. HCHO Removal by MnO₂(x)–CeO₂: Influence of the Synergistic Effect on the Catalytic Activity. *Ind. Eng. Chem. Res.* **2020**, *59*, 596–608. [[CrossRef](#)]
94. Davo-Quinero, A.; Bailon-Garcia, E.; Lopez-Rodriguez, S.; Juan-Juan, J.; Lozano-Castello, D.; Garcia-Melchor, M.; Herrera, F.C.; Pellegrin, E.; Escudero, C.; Bueno-Lopez, A. Insights into the Oxygen Vacancy Filling Mechanism in CuO/CeO₂ Catalysts: A Key Step Toward High Selectivity in Preferential CO Oxidation. *ACS Catal.* **2020**, *10*, 6532–6545. [[CrossRef](#)]
95. Li, F.; Zhao, B.; Tan, Y.; Chen, W.; Tian, M. Preparation of Al₂O₃–CeO₂ by Hydrothermal Method Supporting Copper Oxide for the Catalytic Oxidation of CO and C₃H₈. *Ind. Eng. Chem. Res.* **2022**, *61*, 4739–4751. [[CrossRef](#)]
96. Zhang, J.; Wu, K.; Xiong, J.; Ren, Q.; Zhong, J.; Cai, H.; Huang, H.; Chen, P.; Wu, J.; Chen, L.; et al. Static and Dynamic Quantification Tracking of Asymmetric Oxygen Vacancies in Copper-Ceria Catalysts with Superior Catalytic Activity. *Appl. Catal. B Environ.* **2022**, *316*, 121620. [[CrossRef](#)]
97. Sun, P.; Wang, W.; Dai, X.; Weng, X.; Wu, Z. Mechanism study on catalytic oxidation of chlorobenzene over Mn_xCe_{1–x}O₂/H-ZSM5 catalysts under dry and humid conditions. *Appl. Catal. B Environ.* **2016**, *198*, 389–397. [[CrossRef](#)]
98. Dong, J.; Li, D.; Zhang, Y.; Chang, P.; Jin, Q. Insights into the CeO₂ facet-depended performance of propane oxidation over Pt–CeO₂ catalysts. *J. Catal.* **2022**, *407*, 174–185. [[CrossRef](#)]
99. Zhang, J.; Sun, B.; Guan, X.; Wang, H.; Bao, H.; Huang, Y.; Qiao, J.; Zhou, G. Ruthenium nanoparticles supported on CeO₂ for catalytic permanganate oxidation of butylparaben. *Environ. Sci. Technol.* **2013**, *47*, 13011–13019. [[CrossRef](#)] [[PubMed](#)]
100. Wei, X.; Li, K.; Zhang, X.; Tong, Q.; Ji, J.; Cai, Y.; Gao, B.; Zou, W.; Dong, L. CeO₂ nanosheets with anion-induced oxygen vacancies for promoting photocatalytic toluene mineralization: Toluene adsorption and reactive oxygen species. *Appl. Catal. B Environ.* **2022**, *317*, 121694. [[CrossRef](#)]
101. Kumar, A.; Prasad, B. Catalytic peroxidation of acrylonitrile aqueous solution by Ni-doped CeO₂ catalysts: Characterization, kinetics and thermodynamics. *Int. J. Environ. Sci. Technol.* **2020**, *17*, 1809–1824. [[CrossRef](#)]
102. Wei, X.; Wang, S.; Ni, C.; Wang, M.; Wang, S. Trade-off between redox ability and reactive behaviors for acrylonitrile selective catalytic combustion over the Cu–Ce-based UZM-9 catalysts. *Appl. Catal. A Gen.* **2021**, *610*, 117960. [[CrossRef](#)]
103. Yi, Z.; Sun, J.; Li, J.; Yang, Y.; Zhou, T.; Wei, S.; Zhu, A. The highly efficient removal of HCN over Cu₈Mn₂/CeO₂ catalytic material. *RSC Adv.* **2021**, *11*, 8886–8896. [[CrossRef](#)]
104. Wen, M.; Dong, F.; Yao, J.; Tang, Z.; Zhang, J. Pt nanoparticles confined in the ordered mesoporous CeO₂ as a highly efficient catalyst for the elimination of VOCs. *J. Catal.* **2022**, *412*, 42–58. [[CrossRef](#)]
105. Maurer, F.; Beck, A.; Jelic, J.; Wang, W.; Mangold, S.; Stehle, M.; Wang, D.; Dolcet, P.; Gänzler, A.M.; Kübel, C.; et al. Surface Noble Metal Concentration on Ceria as a Key Descriptor for Efficient Catalytic CO Oxidation. *ACS Catal.* **2022**, *12*, 2473–2486. [[CrossRef](#)]
106. Wang, Q.; Yeung, K.L.; Banares, M.A. Ceria and its related materials for VOC catalytic combustion: A review. *Catal. Today* **2020**, *356*, 141–154. [[CrossRef](#)]

107. Fino, D.; Bensaïd, S.; Piumetti, M.; Russo, N. A review on the catalytic combustion of soot in Diesel particulate filters for automotive applications: From powder catalysts to structured reactors. *Appl. Catal. A* **2016**, *509*, 75–96. [CrossRef]
108. Zheng, C.; Mao, D.; Xu, Z.; Zheng, S. Strong Ru-CeO₂ interaction boosts catalytic activity and stability of Ru supported on CeO₂ nanocube for soot oxidation. *J. Catal.* **2022**, *411*, 122–134. [CrossRef]
109. Jampaiah, D.; Velisoju, V.K.; Devaiah, D.; Singh, M.; Mayes, E.L.H.; Coyle, V.E.; Reddy, B.M.; Bansal, V.; Bhargava, S.K. Flower-like Mn₃O₄/CeO₂ microspheres as an efficient catalyst for diesel soot and CO oxidation: Synergistic effects for enhanced catalytic performance. *Appl. Surf. Sci.* **2019**, *473*, 209–221. [CrossRef]
110. Zhao, H.; Li, H.; Pan, Z.; Feng, F.; Gu, Y.; Du, J.; Zhao, Y. Design of CeMnCu ternary mixed oxides as soot combustion catalysts based on optimized Ce/Mn and Mn/Cu ratios in binary mixed oxides. *Appl. Catal. B Environ.* **2020**, *268*, 118422. [CrossRef]
111. Liu, S.; Wu, X.; Weng, D.; Ran, R. Ceria-based catalysts for soot oxidation: A review. *J. Rare Earths* **2015**, *33*, 567–590. [CrossRef]
112. Guillén-Hurtado, N.; Giménez-Mañogil, J.; Martínez-Munuera, J.C.; Bueno-López, A.; García-García, A. Study of Ce/Pr ratio in ceria-praseodymia catalysts for soot combustion under different atmospheres. *Appl. Catal. A Gen.* **2020**, *590*, 117339. [CrossRef]
113. Fahed, S.; Pointecouteau, R.; Aouine, M.; Boréave, A.; Gil, S.; Meille, V.; Bazin, P.; Toulemonde, O.; Demourgues, A.; Daturi, M.; et al. Pr-rich Cerium-zirconium-praseodymium Mixed Oxides for Automotive Exhaust Emission Control. *Appl. Catal. A Gen.* **2022**, *644*, 118800. [CrossRef]
114. Levasseur, B.; Kaliaguine, S. Effects of iron and cerium in La_{1–y}Ce_yCo_{1–x}FexO₃ perovskites as catalysts for VOC oxidation. *Appl. Catal. B Environ.* **2009**, *88*, 305–314. [CrossRef]
115. Zhang, J.; Nazarenko, Y.; Zhang, L.; Calderon, L.; Lee, K.-B.; Garfunkel, E.; Schwander, S.; Tetley, T.D.; Chung, K.F.; Porter, A.E.; et al. Impacts of a Nanosized Ceria Additive on Diesel Engine Emissions of Particulate and Gaseous Pollutants. *Environ. Sci. Technol.* **2013**, *47*, 13077–13085. [CrossRef] [PubMed]
116. Wakefield, G.; Wu, X.; Gardener, M.; Park, B.; Anderson, S. Envirox™ fuel-borne catalyst: Developing and launching a nano-fuel additive. *Technol. Anal. Strateg. Manag.* **2008**, *20*, 127–136. [CrossRef]
117. Cerion Energy's Ground Breaking GO2 Diesel Fuel Additive Wins Most ECO-Friendly Product in the DAME Awards 2011. Available online: http://www.nanotech-now.com/news.cgi?story_id=43885 (accessed on 16 June 2022).
118. Roos, J.W.; Richardson, D.; Claydon, D.J. Diesel Fuel Additives Containing Cerium or Manganese and Detergents. U.S. Patent Application 20080066375, 20 March 2008.
119. Difrancesco, A.G.; Hailstone, R.K.; Langner, A.; Reed, K.J. Cerium Dioxide Nanoparticle Manufacture for Use as Combustion Improvers in Diesel Fuel and Biodiesel. WO2008030815, 13 March 2008.
120. Lin, K.-S.; Chowdhury, S. Synthesis, characterization, and application of 1-D cerium oxide nanomaterials: A review. *Int. J. Mol. Sci.* **2010**, *11*, 3226–3251. [CrossRef] [PubMed]
121. So, Y.-M.; Leung, W.-H. Recent advances in the coordination chemistry of cerium(IV) complexes. *Coord. Chem. Rev.* **2017**, *340*, 172–197. [CrossRef]
122. Zhu, M.; Lai, J.-K.; Tumuluri, U.; Ford, M.E.; Wu, Z.; Wachs, I.E. Reaction Pathways and Kinetics for Selective Catalytic Reduction (SCR) of Acidic NO_x Emissions from Power Plants with NH₃. *ACS Catal.* **2017**, *7*, 8358–8361. [CrossRef]
123. Cao, X.; Zhang, C.; Dong, F.; Sun, X. Mechanistic insight into the selective catalytic reduction of NO_x with propene on the Ce_{0.875}Zr_{0.125}O₂ (110) surface. *Catal. Sci. Technol.* **2022**, *12*, 3685–3694. [CrossRef]
124. Krocher, O. Selective Catalytic Reduction of NO_x. *Catalysts* **2018**, *8*, 459. [CrossRef]
125. Guan, B.; Zhan, R.; Lin, H.; Huang, Z. Review of state of the art technologies of selective catalytic reduction of NO_x from diesel engine exhaust. *Appl. Therm. Eng.* **2014**, *66*, 395–414. [CrossRef]
126. Huang, X.; Zhang, G.; Lu, G.; Tang, Z. Recent Progress on Establishing Structure–Activity Relationship of Catalysts for Selective Catalytic Reduction (SCR) of NO_x with NH₃. *Catal. Surv. Asia* **2018**, *22*, 1–19. [CrossRef]
127. Zhang, J.; Li, X.; Chen, P.; Zhu, B. Research Status and Prospect on Vanadium-Based Catalysts for NH₃-SCR Denitration. *Materials* **2018**, *11*, 1632. [CrossRef]
128. Shan, W.; Liu, F.; Yu, Y.; He, H. The use of ceria for the selective catalytic reduction of NO_x with NH₃. *Chin. J. Catal.* **2014**, *35*, 1251–1259. [CrossRef]
129. Chen, L.; Si, Z.; Wu, X.; Weng, D.; Ran, R.; Yu, J. Rare earth containing catalysts for selective catalytic reduction of NO_x with ammonia: A Review. *J. Rare Earths* **2014**, *32*, 907–917. [CrossRef]
130. Hu, W.; Zou, R.; Dong, Y.; Zhang, S.; Song, H.; Liu, S.; Zheng, C.; Nova, I.; Tronconi, E.; Gao, X. Synergy of vanadia and ceria in the reaction mechanism of low-temperature selective catalytic reduction of NO_x by NH₃. *J. Catal.* **2020**, *391*, 145–154. [CrossRef]
131. Peng, Y.; Wang, C.; Li, J. Structure–activity relationship of VO_x/CeO₂ nanorod for NO removal with ammonia. *Appl. Catal. B Environ.* **2014**, *144*, 538–546. [CrossRef]
132. Chen, L.; Li, J.; Ge, M. Promotional Effect of Ce-doped V₂O₅-WO₃/TiO₂ with Low Vanadium Loadings for Selective Catalytic Reduction of NO_x by NH₃. *J. Phys. Chem. C* **2009**, *113*, 21177–21184. [CrossRef]
133. Cai, M.; Bian, X.; Xie, F.; Wu, W.; Cen, P. Preparation and performance of cerium-based catalysts for selective catalytic reduction of nitrogen oxides: A critical review. *Catalysts* **2021**, *11*, 361. [CrossRef]
134. Xu, J.; Yu, H.; Zhang, C.; Guo, F.; Xie, J. Development of cerium-based catalysts for selective catalytic reduction of nitrogen oxides: A review. *New J. Chem.* **2019**, *43*, 3996–4007. [CrossRef]
135. Wu, X.; Yu, X.; Huang, Z.; Shen, H.; Jing, G. MnO_x-decorated VO_x/CeO₂ catalysts with preferentially exposed {110} facets for selective catalytic reduction of NO_x by NH₃. *Appl. Catal. B Environ.* **2020**, *268*, 118419. [CrossRef]

136. Sun, H.; Park, S.-J. Recent Advances in $\text{MnO}_x/\text{CeO}_2$ -Based Ternary Composites for Selective Catalytic Reduction of NO_x by NH_3 : A Review. *Catalysts* **2021**, *11*, 1519. [CrossRef]
137. Andana, T.; Rappé, K.G.; Nelson, N.C.; Gao, F.; Wang, Y. Selective catalytic reduction of NO_x with NH_3 over Ce-Mn oxide and Cu-SSZ-13 composite catalysts—Low temperature enhancement. *Appl. Catal. B Environ.* **2022**, *316*, 121522. [CrossRef]
138. Zhu, Q.; Wang, A.; Zhang, J.; Guo, Y.; Guo, Y.; Wang, L.; Zhan, W. Low-Temperature NH_3 -SCR on Cex-Mn-Tiy Mixed Oxide Catalysts: Improved Performance by the Mutual Effect between Ce and Ti. *Catalysts* **2022**, *12*, 471. [CrossRef]
139. Zhou, J.; Guo, R.-T.; Zhang, X.-F.; Liu, Y.-Z.; Duan, C.-P.; Wu, G.-L.; Pan, W.-G. Cerium Oxide-Based Catalysts for Low-Temperature Selective Catalytic Reduction of NO_x with NH_3 : A Review. *Energy Fuels* **2021**, *35*, 2981–2998. [CrossRef]
140. Tang, C.; Zhang, H.; Dong, L. Ceria-based catalysts for low-temperature selective catalytic reduction of NO with NH_3 . *Catal. Sci. Technol.* **2016**, *6*, 1248–1264. [CrossRef]
141. Zhou, Q.; He, K.; Wang, X.; Lim, K.H.; Liu, P.; Wang, W.; Wang, Q. Investigation on the redox/acidic features of bimetallic MOF-derived CeMO_x catalysts for low-temperature NH_3 -SCR of NO_x . *Appl. Catal. A Gen.* **2022**, *643*, 118796. [CrossRef]
142. Yang, S.; Kim, M.; Yang, S.; Kim, D.S.; Lee, W.J.; Lee, H. Production of acrylic acid from biomass-derived allyl alcohol by selective oxidation using Au/ceria catalysts. *Catal. Sci. Technol.* **2016**, *6*, 3616–3622. [CrossRef]
143. Available online: <https://cen.acs.org/articles/88/i21/Arkema-Pushes-Biobased-Acrylics.html> (accessed on 25 August 2022).
144. A Plant-Based Solution. Available online: <https://www.adm.com/en-us/products-services/industrial-biosolutions/products/propylene-glycol> (accessed on 6 July 2022).
145. Mai, H.-X.; Sun, L.-D.; Zhang, Y.-W.; Si, R.; Feng, W.; Zhang, H.-P.; Liu, H.-C.; Yan, C.-H. Shape-Selective Synthesis and Oxygen Storage Behavior of Ceria Nanopolyhedra, Nanorods, and Nanocubes. *J. Phys. Chem. B* **2005**, *109*, 24380–24385. [CrossRef]
146. Smith, L.R.; Sainna, M.A.; Douthwaite, M.; Davies, T.E.; Dummer, N.F.; Willock, D.J.; Knight, D.W.; Catlow, C.R.A.; Taylor, S.H.; Hutchings, G.J. Gas Phase Glycerol Valorization over Ceria Nanostructures with Well-Defined Morphologies. *ACS Catal.* **2021**, *11*, 4893–4907. [CrossRef]
147. Dimitratos, N.; Lopez-Sanchez, J.A.; Hutchings, G.J. Green Catalysis with Alternative Feedstocks. *Top. Catal.* **2009**, *52*, 258–268. [CrossRef]
148. Miedziak, P.J.; Alshammari, H.; Kondrat, S.A.; Clarke, T.J.; Davies, T.E.; Morad, M.; Morgan, D.J.; Willock, D.J.; Knight, D.W.; Taylor, S.H.; et al. Base-free glucose oxidation using air with supported gold catalysts. *Green Chem.* **2014**, *16*, 3132–3141. [CrossRef]
149. Albrecht, K.; Brazdil, J. Processes for Preparing Aldaric, Aldonic, and Uronic Acids. WO2021101810, 27 May 2021.
150. Qi, X.; He, Y.; Yao, Y.; Li, Y.; Zhang, L.; Geng, M.; Wei, H.; Chu, H. Effect of CeO_2 morphology on the catalytic properties of Au/ CeO_2 for base-free glucose oxidation. *Catal. Sci. Technol.* **2022**, *12*, 1313–1323. [CrossRef]
151. Ventura, M.; Lobefaro, F.; de Giglio, E.; Distaso, M.; Nocito, F.; Dibenedetto, A. Selective Aerobic Oxidation of 5-Hydroxymethylfurfural to 2,5-Diformylfuran or 2-Formyl-5-furancarboxylic Acid in Water by using $\text{MgO}\cdot\text{CeO}_2$ Mixed Oxides as Catalysts. *ChemSusChem* **2018**, *11*, 1305–1315. [CrossRef] [PubMed]
152. Han, X.; Li, C.; Liu, X.; Xia, Q.; Wang, Y. Selective oxidation of 5-hydroxymethylfurfural to 2,5-furandicarboxylic acid over $\text{MnO}_x\text{-CeO}_2$ composite catalysts. *Green Chem.* **2017**, *19*, 996–1004. [CrossRef]
153. Gao, P.; Kang, Z.; Fu, W.; Wang, W.; Bai, X.; Wang, E. Electrically Driven Redox Process in Cerium Oxides. *J. Am. Chem. Soc.* **2010**, *132*, 4197–4201. [CrossRef]
154. Yashima, M.; Hirose, T.; Katano, S.; Suzuki, Y.; Kakihana, M.; Yoshimura, M. Structural changes of $\text{ZrO}_2\text{-CeO}_2$ solid solutions around the monoclinic-tetragonal phase boundary. *Phys. Rev. B Condens. Matter* **1995**, *51*, 8018. [CrossRef] [PubMed]
155. Van den Elzen, A.F.; Rieck, G.D. The crystal structure of $\text{Bi}_2(\text{MoO}_4)_3$. *Acta Crystallogr. Sect. B* **1973**, *29*, 2433–2436. [CrossRef]
156. Brixner, L.H.; Sleight, A.W.; Licitis, M.S. Cell dimensions of the molybdates $\text{La}_2(\text{MoO}_4)_3$, $\text{Ce}_2(\text{MoO}_4)_3$, $\text{Pr}_2(\text{MoO}_4)_3$, and $\text{Nd}_2(\text{MoO}_4)_3$. *J. Solid State Chem.* **1972**, *5*, 247–249. [CrossRef]
157. Brazdil, J.F. Scheelite: A versatile structural template for selective alkene oxidation catalysts. *Catal. Sci. Technol.* **2015**, *5*, 3452–3458. [CrossRef]
158. Brazdil, J.F.; Toft, M.A.; Lin, S.S.Y.; McKenna, S.T.; Zajac, G.; Kaduk, J.A.; Golab, J.T. Characterization of bismuth–cerium–molybdate selective propylene ammoxidation catalysts. *Appl. Catal. A Gen.* **2015**, *495*, 115–123. [CrossRef]
159. Graciani, J.; Mudiyansele, K.; Xu, F.; Baber Ashleigh, E.; Evans, J.; Senanayake Sanjaya, D.; Stacchiola Darío, J.; Liu, P.; Hrbek, J.; Sanz Javier, F.; et al. Highly active copper-ceria and copper-ceria-titania catalysts for methanol synthesis from CO_2 . *Science* **2014**, *345*, 546–550. [CrossRef]
160. Vayssilov, G.N.; Lykhach, Y.; Migani, A.; Staudt, T.; Petrova, G.P.; Tsud, N.; Skála, T.; Bruix, A.; Illas, F.; Prince, K.C.; et al. Support nanostructure boosts oxygen transfer to catalytically active platinum nanoparticles. *Nat. Mater.* **2011**, *10*, 310–315. [CrossRef]
161. Cargnello, M.; Doan-Nguyen, V.V.T.; Gordon, T.R.; Diaz, R.E.; Stach, E.A.; Gorte, R.J.; Fornasiero, P.; Murray, C.B. Control of Metal Nanocrystal Size Reveals Metal-Support Interface Role for Ceria Catalysts. *Science* **2013**, *341*, 771–773. [CrossRef] [PubMed]
162. Zolotova, E.S.; Trushnikova, L.N.; Ayupov, B.M.; Sokolov, V.V.; Daletskii, V.A. $\text{Na}_2\text{MoO}_4\text{-CaMoO}_4\text{-Ce}_{2/3}\text{MoO}_4$ scheelite-like solid solutions. *Inorg. Mater.* **2009**, *45*, 432–435. [CrossRef]
163. Kruth, A.; Mather, G.C.; Jurado, J.R.; Irvine, J.T.S. Anomalous variations of unit cell parameters with composition in proton conducting, ACeO_3 -type perovskite solid solutions. *Solid State Ion.* **2005**, *176*, 703–712. [CrossRef]
164. Varez, A.; Garcia-Gonzalez, E.; Sanz, J. Cation miscibility in $\text{CeO}_2\text{-ZrO}_2$ oxides with fluorite structure. A combined TEM, SAED and XRD Rietveld analysis. *J. Mater. Chem.* **2006**, *16*, 4249–4256. [CrossRef]

165. Tian, F. A Review of Solid-Solution Models of High-Entropy Alloys Based on Ab Initio Calculations. *Front. Mater.* **2017**, *4*, 36. [[CrossRef](#)]
166. Stenzel, D.; Issac, I.; Wang, K.; Azmi, R.; Singh, R.; Jeong, J.; Najib, S.; Bhattacharya, S.S.; Hahn, H.; Brezesinski, T.; et al. High Entropy and Low Symmetry: Triclinic High-Entropy Molybdates. *Inorg. Chem.* **2021**, *60*, 115–123. [[CrossRef](#)]
167. Gao, Y.; Liu, Y.; Yu, H.; Zou, D. High-entropy oxides for catalysis: Status and perspectives. *Appl. Catal. A Gen.* **2022**, *631*, 118478. [[CrossRef](#)]
168. Zheng, Z.; Ji, H.; Zhang, Y.; Cai, J.; Mo, C. High-entropy $(\text{Ca}_{0.5}\text{Ce}_{0.5})(\text{Nb}_{0.25}\text{Ta}_{0.25}\text{Mo}_{0.25}\text{W}_{0.25})\text{O}_4$ scheelite ceramics with high-temperature negative temperature coefficient (NTC) property for thermistor materials. *Solid State Ion.* **2022**, *377*, 115872. [[CrossRef](#)]
169. Zhu, D.; Liu, H.; Huang, Y.; Luo, X.; Mao, Y.; Liang, Z. Study of Direct Synthesis of DMC from CO_2 and Methanol on CeO_2 : Theoretical Calculation and Experiment. *Ind. Eng. Chem. Res.* **2022**. [[CrossRef](#)]
170. Ogada, J.J.; Ipadeola, A.K.; Mwonga, P.V.; Haruna, A.B.; Nichols, F.; Chen, S.; Miller, H.A.; Pagliaro, M.V.; Vizza, F.; Varcoe, J.R.; et al. CeO_2 Modulates the Electronic States of a Palladium Onion-Like Carbon Interface into a Highly Active and Durable Electrocatalyst for Hydrogen Oxidation in Anion-Exchange-Membrane Fuel Cells. *ACS Catal.* **2022**, *12*, 7014–7029. [[CrossRef](#)]
171. Ji, G.; Zhao, L.; Wang, Y.; Tang, Y.; He, C.; Liu, S.; Duan, C. A Binuclear Cerium-Based Metal–Organic Framework as an Artificial Monooxygenase for the Saturated Hydrocarbon Aerobic Oxidation with High Efficiency and High Selectivity. *ACS Catal.* **2022**, *12*, 7821–7832. [[CrossRef](#)]
172. Zoller, S.; Koepf, E.; Nizamian, D.; Stephan, M.; Patané, A.; Haueter, P.; Romero, M.; González-Aguilar, J.; Lieftink, D.; de Wit, E.; et al. A solar tower fuel plant for the thermochemical production of kerosene from H_2O and CO_2 . *Joule* **2022**, *6*, 1606–1616. [[CrossRef](#)] [[PubMed](#)]
173. Solar-Powered Reactor Converts CO_2 and Water into Jet Fuel. Available online: <https://cendigitalmagazine.acs.org/2022/08/01/solar-powered-reactor-converts-co%E2%82%82-and-water-into-jet-fuel/content.html> (accessed on 3 August 2022).